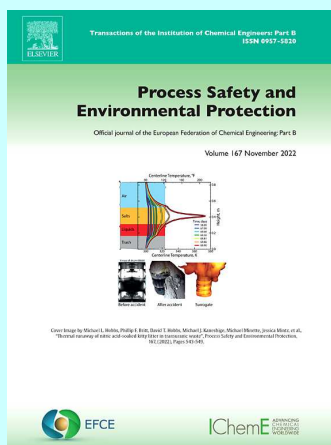


# Process Safety and Environmental Protection

Rok 2022, Volume 165

September



**Fang Qi, Jian Sun, Ganyu Zhu, Huiquan Li, Yongji Wu, Shaopeng Li, Chennian Yang, Jun Zheng, Yimin Zhang. *Recycling of blast furnace slag to prepare calcium silicate hydrate by mechano-chemical co-activation and its application to calcium silicate fireproof board. Pages 1-12.***

The high-value utilization of water quenched slag (WQS), one of the bulk byproducts originating from the iron manufacturing industry, remains an important subject in the environment. Through a mechano-chemical co-activation strategy, WQS can be used to prepare porous calcium silicate hydrate (C-S-H), which was applied as gelling filler to prepare fiber-reinforced calcium silicate fireproof board (FCSFB) and extremely improved its high-temperature performance and non-combustibility. The optimal activation conditions for WQS are ball milling time of 30 min, reaction temperature of 90 °C, reaction time of 5 h, and Ca/Si molar ratio of 1.5:1. The thermal conductivity for FCSFB prepared by the optimal A-WQS is 0.17 W/(m•K), and its overheating time of the applied temperature at 803.7 °C is 1335.5 s. The improvement mechanism of the performance of FCSFB can be attributed to the transformation of C-S-H toward more high crystallinity flaky tobermorite, which uniformly and closely combined with pulp fiber to form a micro-porous cavity structure to delay flame penetration period. The application of WQS in FCSFB can provide essential guidance for the utilization of other similar solid wastes.

- **Keywords:** Calcium silicate hydrate; Calcium silicate fireproof board; Water quenched slag; Mechano-chemical co-activation

**Jing Wen, Tangxia Yu, Tao Jiang, Hongyan Sun, Ming Li, Yi Peng. *Effect of chromium content on the phase composition, crystallization and components extraction of vanadium slag. Pages 13-21.***

The existence of chromium in vanadium slag is generally considered to affect its phase composition, micromorphology, and further vanadium extraction by calcification roasting process. In this work, remelting and crystallization were used to prepare vanadium slag with different Cr<sub>2</sub>O<sub>3</sub> mass fractions. The aforementioned effects were then examined through X-ray diffraction, scanning electron microscope, and leaching experiments.

Results showed that Cr<sub>2</sub>O<sub>3</sub> content affects spinel phase in vanadium slag. With the increase in Cr<sub>2</sub>O<sub>3</sub> content, chromium was observed in the (Mn, Fe)(V, Cr)<sub>2</sub>O<sub>4</sub> phase with vanadium in a homogeneous form, while the diffraction peak positions of (Mn, Fe)(V, Cr)<sub>2</sub>O<sub>4</sub> shifted by a large angle from the lattice distortion. Further, the average grain size of spinel gradually decreased because of the increase in the number of crystallization centers, and the distribution of Cr, V, and Ti in the spinel phase were gradually homogenized instead of having obvious stratification. After calcification roasting, vanadium and chromium existed in the form of vanadate and (Fe<sub>0.6</sub>Cr<sub>0.4</sub>)<sub>2</sub>O<sub>3</sub>, achieving the complete separation of them after acid leaching. The increase in Cr<sub>2</sub>O<sub>3</sub> content had no significant effect on the leaching behavior of vanadium. Additionally, increasing the roasting temperature and accelerating the heating process contributed to restraining chromium extraction. These results provide a research basis for the resource utilization of vanadium slag and vanadium chromium slag.

- **Keywords:** Vanadium slag; Chromium content; Phase composition; Crystallization; Calcification roasting; Cr (VI)

**Dmitri Nikitin, Balpreet Kaur, Sergei Preis, Niina Dulova. *Persulfate contribution to photolytic and pulsed corona discharge oxidation of metformin and tramadol in water.* Pages 22-30.**

Degradation and mineralization of antidiabetic metformin (MTF) and opioid tramadol (TMD) in water were studied in UV photolytic oxidation and pulsed corona discharge (PCD) combined with extrinsic persulfate (PS) as UV/PS and PCD/PS systems. The effect of PS dose variation on the oxidation rate and efficiency was assessed. The UV/PS combination showed considerable effect in MTF and TMD removal, enhancing the removal of TOC up to 60–65% at maximum applied PS dose, thus providing the highest cost efficiency. As for the PCD/PS oxidation, the synergy was noticed for MTF, moderately increasing the oxidation rate and mineralization at somewhat increased expense. The PS addition to PCD treatment, however, demonstrated no effect on TMD oxidation. The highest energy efficiency in MTF and TMD degradation was thus showed by non-assisted PCD treatment with an energy yield at 90% conversion of the target compound of 5.6 and 13 g kW<sup>-1</sup> h<sup>-1</sup>, respectively, confirming its practical applicability. The effective mineralization of the target compounds in persulfate photolysis makes it promising for use in advanced water purification. To assess the environmental safety of the studied oxidation processes, the acute toxicity of the treated MTF and TMD solutions to luminous bacteria (*Vibrio fischeri*) was examined.

- **Keywords:** Advanced oxidation; Pharmaceuticals; Photolysis; Peroxydisulfate; Electric discharge; Plasma

**Krantiraditya Dhalmahapatra, Abhishek Verma, J. Maiti. *An integrated TRIZ coupled safety function deployment and capital budgeting methodology for occupational safety improvement: A case of manufacturing industry.* Pages 31-45.**

In this study, a novel scheme is proposed for occupational safety improvement by leveraging the concepts of Virtual Reality (VR), Safety Function Deployment (SFD), TRIZ (theory of inventive problem solving) and capital budgeting approach. This integrated approach helped in identifying safety interventions, which added a new dimension to the safety intervention design in the operational study at the workplace. By observing the effectiveness of the immersive safety training in identifying the accident path elements such as hazards and initiating mechanisms, a three-dimensional (3D) VR environment is created for safety training of Electric Overhead Travelling (EOT) crane operators of the studied manufacturing industry. This study is carried out in two phases based on accident path elements identified before and after safety training in the VR platform. Three House

of Safety (HoSs) are used in this study to establish a relationship between tasks and hazards, hazards and initiating mechanism, and initiating mechanism and safety interventions. Priority weight of interventions in the last HoS is fed as input to the capital budgeting methodology for the selection of an optimal number of interventions for safety improvement. 0–1 multi-dimensional knapsack model is used in capital budgeting considering safety budget and cost of each intervention. We have introduced Z- number approach in capital budgeting methodology to characterize the reliability of experts' opinion considered in this process. A 15% improvement in safety performance is observed after safety training. Further, it is observed that technology-based interventions (laser scanner, smart helmet, smart jacket, Radio Frequency Identification (RFID) to monitor Personal Protective Equipment (PPE), immersive safety training) are having more weightage than traditional safety interventions after safety training.

- **Keywords:** Occupational safety; Safety training; Virtual reality; Intervention design; 0–1 multi-dimensional knapsack

**Ruming Pan, Gérald Debenest, Marco A.B. Zanoni. *Numerical study of plastic waste pyrolysis driven by char smoldering.* Pages 46-56.**

Pyrolysis is a promising process for the valorization of plastic waste (PW). However, traditional pyrolysis processes have high energy consumption. On the other hand, smoldering has been proven as an effective and economic process to treat waste, becoming an attractive application for developing countries. Therefore, a reactor for PW pyrolysis driven by char smoldering was investigated in this study. A proof-of-concept was the development of a multidimensional mathematical model to verify the proposed reactor's feasibility and evaluate its performance. It was found that PW was pyrolyzed stably driven by a self-sustaining char smoldering front. The model suggested that the air inlet velocity and char concentration determined the duration of the PW pyrolysis process and tar and gas yields by regulating the front velocity and the peak temperature. The carrier gas inlet velocity controlled the tar's residence time in the PW pyrolysis chamber and further affected the tar and gas yields.

- **Keywords:** Smoldering; Char; Pyrolysis; Plastic waste; Multidimensional model; Tar

**Banu Taşkan, Ergin Taşkan, Halil Hasar. *New quorum quenching bacteria for controlling biofilm thickness in the membrane aerated biofilm reactor.* Pages 57-65.**

The uncontrolled increase of biofilm thickness on the membrane surface directly affects substrate diffusion rate, pollutant removal efficiency, and microbial ecology of the membrane aerated biofilm reactor (MABR). This study aimed to control the biofilm growth using a promising antifouling strategy called quorum quenching (QQ). For this purpose, new QQ bacteria (*Bacillus methylotrophicus* BT1, *Klebsiella pneumoniae* BT2, *Lysinibacillus fusiformis* BT3, and *Achromobacter xylosoxidans* BT4) were isolated and immobilized to control the biofilm thickness on the membrane fibers in MABR. The *Bacillus methylotrophicus* BT1 with the highest QQ activity disrupted bacterial communication among microorganisms, provided a relatively thin and dense biofilm thickness (250 µm), and exhibited the best MABR performance. The amount of EPS secreted by the microorganisms significantly decreased due to the increase in the QQ activities of the QQ bacteria. A significant COD removal performance improvement of 74.5% compared to the control-MABR was achieved by MABR containing BT1. Microbial analysis revealed a change in the microbial community structure of biofilms in the MABRs containing different QQ bacteria. In conclusion, the newly isolated QQ bacteria effectively could be controlled biofilm formation on the membrane fibers in MABR systems, and the results obtained can form the basis for larger-scale studies.

- **Keywords:** Membrane aerated biofilm reactor (MABR); Quorum quenching (QQ); Isolation of bacteria; Biofilm thickness; Microbial community

**Yingying Duan, Jianhai Zhao, Xiuming Qiu, Xiaoli Deng, Xiaoyu Ren, Wenqi Ge, Hongying Yuan. *Coagulation performance and floc properties for synchronous removal of reactive dye and polyethylene terephthalate microplastics. Pages 66-76.***

As a new type of pollutant, microplastics are widely distributed in printing and dyeing wastewater. Coagulation performance, floc characteristics and mechanisms for synchronous removal of reactive orange and polyethylene terephthalate (PET) microplastics using magnesium hydroxide and polyacrylamide (PAM) were investigated in this paper. The floc properties were evaluated by laser particle size analysis and on line intelligent photometric dispersion analysis. Coagulation mechanism was investigated by scanning electron microscope (SEM), Fourier transform infrared spectroscopy (FTIR) and Zeta analyzer. The results showed that the removal efficiencies for reactive orange and PET were 98 % and 93 % under the optimal conditions of magnesium ion 100 mg/L, PAM 4 mg/L with pH value 11.75. The increase of pH, coagulant and PAM dosage would significantly enhance the removal efficiency. The average floc size reached 61.90  $\mu\text{m}$  and these flocs aggregated together for fast sedimentation. Meanwhile, electrical neutralization and adsorption for reactive orange by magnesium hydroxide, PAM bridging for PET were the main mechanisms. The removal behavior of reactive orange and PET microplastics during coagulation has potential applications for the removal of printing and dyeing wastewater.

- **Keywords:** Magnesium hydroxide; Reactive orange; PET; Coagulation; Mechanism

**Julio Ariel Dueñas Santana, Yanelys Cuba Arana, Orelvis González Gómez, Daniel Furka, Samuel Furka, Jesús Luis Orozco, Almerinda Di Benedetto, Danilo Russo, Maria Portarapillo, Jonathan Serrano Febles. *Fire and Explosion Economic Losses (FEEL) Index: A new approach for quantifying economic damages due to accidents in hydrocarbon storage sites. Pages 77-92.***

One of the areas most affected by the occurrence of fires and explosions is the economy. These accidents lead to direct economic damages, which results in the withdrawal of capital for the reconstruction of damaged areas. In addition, there are other indirect economic losses, such as business interruption and reputational losses. The DOW Fire and Explosion Index (F&EI-DOW) is currently the most complete methodology for quantifying economic losses. Notwithstanding, the F&EI-DOW focuses on quantifying the hazardous potential of process units, and, does not provide an overall criterion for the hazardous potential of the entire industrial site with regard to: the inclusion of the so-called domino effect, the probabilistic risk assessment, the updating of existing risk analysis tools with new emerging Artificial Intelligence Techniques, and the quantification of reputation losses. For this purpose, the development of a new Fire and Explosion Economic Losses-Index (FEEL-Index) is proposed, which integrates the F&EI-DOW with new factors, such as the Damaged Area Factor, the Accident Probability Factor and the Reputation Loss Factor. With regard to the application to a case study, the total losses quantified by the overall FEEL-Index predict a value higher than the one predicted by the F&EI-DOW. The results obtained on an hydrocarbon storage case study show that the application of the FEEL-Index is relevant for increasing the risk perception, as well as providing guidance for prevention, mitigation, and risk management of accidents in process industries.

- **Keywords:** Economic impact; Fire; Explosion; Domino effect; Artificial Intelligence; Risk analysis

**Nannan Geng, Wei Chen, Hang Xu, Mingmei Ding, Zongli Xie, Anqi Wang. *Removal of tetracycline hydrochloride by Z-scheme heterojunction sono-catalyst acting on ultrasound/H<sub>2</sub>O<sub>2</sub> system. Pages 93-101.***

Because of the unique advantages, ultrasound (US) has become a popular technology for water organic treatment. In order to compensate for the disadvantages of expensive equipment and large energy input caused by US, researchers combine US with iron-based sono-catalyst to realize the rapid and efficient degradation of pollutants. Aiming at the ultrasonic hot spot and sonoluminescence effect, in this work, Z-type heterojunction sono-catalyst FeII-MIL-88B/GO/P25 (FeII-MGP) was synthesized for TC-HCl removal. The physicochemical properties of the material were characterized by SEM, XRD, XPS and BET. The addition of GO contributed to the formation of the Z-Scheme heterojunction. At the optimal reaction conditions determined by influential factor experiments (ultrasonic power of 100 W, sono-catalyst dose of 0.3 g/L, H<sub>2</sub>O<sub>2</sub> dose of 20 mM and pH 5), in only 7 min, 83.3 % of TC-HCl was removed, and the TOC degradation efficiency reached 52.2 %. The contrast experiment demonstrated that the US/FeII-MGP/H<sub>2</sub>O<sub>2</sub> system had the best pollutant removal performance. After three repeated experiments, the removal efficiency decreased by only 6 %. ·OH was identified as the major radical from the quenching experiments and technical EPR. UV-vis and Mott-Schottky measurements suggested that the possible carrier transfer paths followed the Z-Scheme heterojunction model.

- **Keywords:** Z-scheme heterojunction; Ultrasound; US/FeII-MGP/H<sub>2</sub>O<sub>2</sub> system; Hot spot; Sonoluminescence

**Yiming Jiang, Xuhai Pan, Min Hua, Tao Zhang, Qingyuan Wang, Zhilei Wang, Yunyu Li, Andong Yu, Juncheng Jiang. *Non-premixed flame propagation inside and outside the different three-way tubes after the self-ignition of pressurized hydrogen. Pages 102-113.***

Accidental leakage of pressurized hydrogen into the pipeline is often accompanied by the non-premixed self-ignition flame, whilst the complex structure of pipeline affects the flame propagation. In this study, the propagation of self-ignition hydrogen flame in different three-way tubes is studied and the flame evolution near the two exits is compared. Effects of the tube length and the location of bifurcation points are investigated. Results show that the bifurcation structure has the attenuation effect on the intensity of flame and shock wave, and they attenuate more sharply in the branch pipeline. But the flame intensity can increase again downstream the bifurcation point in the trunk pipeline, and this increase is not continuous and decrease again as the tube length increases. In addition, the flame evolution can be different near two exits of the tube. As the bifurcation point moves downstream, the number of Mach disk and the time required to form the stable flame will increase near the exit of branch pipeline. Despite different flame evolution, the flame morphology and propagation are all controlled by the shock wave structures before the formation of the vortex, but the flame changes dramatically and grows rapidly to form the stable lift-off flame after the formation of the vortex.

- **Keywords:** Hydrogen safety; Self-ignition; Non-premixed flame propagation; Three-way tube; Shock wave

**Yiping Bai, Jiansong Wu, Shuaiqi Yuan, Genserik Reniers, Ming Yang, Jitao Cai. *Dynamic resilience assessment and emergency strategy optimization of natural gas compartments in utility tunnels. Pages 114-125.***

As a kind of critical infrastructure of energy transportation, so-called 'utility tunnels' have been developed around the world. Hosting a natural gas pipeline inside the natural gas compartment of a utility tunnel facilitates its maintenance but also brings potential explosion concerns due to the confined space. Although some work focuses on the risk analysis of the natural gas pipeline inside utility tunnels, a resilience assessment is needed for dynamically modeling leakage with interacting safety barriers. In this paper, a resilience assessment model of the natural gas compartment of utility tunnels is elaborated based on numerical simulation considering interacting barrier modeling, including sensors, a ventilation system, and the possibility of emergency shutdown. Based on the calculated (natural gas compartment) resilience for casualty and economic loss, ventilation strategies and sensor layouts can be recommended and optimization is possible. Meanwhile, the delay effect of safety barriers is investigated in this work, and the unequal interval layouts of sensors are explored and proven to be effective without any further cost. The proposed resilience assessment model can be important to further improve the safety management of utility tunnels and other confined spaces where hazardous gases are transported.

- **Keywords:** Resilience assessment; Utility tunnel; Natural gas; Safety barrier; Emergency strategy optimization

**Christopher Muller, Karla Guevarra, Amanda Summers, Laurie Pierce, Parisa Shahbaz, Peter Edwin Zemke, Karina Woodland, Vicky Hollingsworth, George Nakhla, Kati Bell, Embrey Bronstad. *A review of the practical application of micro-aeration and oxygenation for hydrogen sulfide management in anaerobic digesters. Pages 126-137.***

With the increased use of biogas generated from anaerobic digestion (AD) as a source of renewable energy, economical methods of cleaning and upgrading the gas are of growing importance. The removal of hydrogen sulfide to varying degrees is required regardless of the end biogas use, as the presence of hydrogen sulfide contributes to operations and maintenance costs and reduction in the life of gas handling equipment. Micro-aeration, or the injection of small amounts of oxygen, into anaerobic digesters has been shown to affect reduction in gaseous hydrogen sulfide concentrations and is more economical than typical sulfide scrubbing systems. This review examines the existing data on micro-aeration applications, including biological kinetics and appropriate control strategies for full-scale micro-aeration applications. Knowledge gaps in research are also noted.

- **Keywords:** Micro-aeration; Micro-oxygenation; Hydrogen sulfide oxidation; Sulfide oxidizing bacteria (SOB); Anaerobic digestion; Biogas

**Haobin Wang, Baiqiang Zhang, Huiping Yang, Qiang Bao, Bo Wu. *New insights on the effects of SO<sub>2</sub> on NO oxidation from flue gas with H<sub>2</sub>O<sub>2</sub> vapor over Fe<sub>2</sub>O<sub>3</sub>/SiO<sub>2</sub>. Pages 138-150.***

The positive effects of SO<sub>2</sub> on NO oxidation with H<sub>2</sub>O<sub>2</sub> vapor over a Fe<sub>2</sub>O<sub>3</sub>/SiO<sub>2</sub> catalyst were investigated. In well-designed experiments, the pretreatment of S-contained gaseous species and NO oxidation were carried out. The results indicated that the sulfate species from the oxidation of SO<sub>2</sub> could significantly promote NO oxidation. In the radical scavenger and ESR tests, the H<sub>2</sub>O<sub>2</sub> decomposition over SO<sub>2</sub>-pretreated Fe<sub>2</sub>O<sub>3</sub>/SiO<sub>2</sub> produced •OH and •SO<sub>4</sub><sup>-</sup>. The •OH was dominant for NO oxidation. The XPS tests verified the Fe(III) reduction and the surface SO<sub>4</sub><sup>2-</sup> species formation on Fe<sub>2</sub>O<sub>3</sub>/SiO<sub>2</sub>.

According to the kinetic studies, the NO adsorbed Eley-Rideal model gave the best fit, indicating that the adsorbed NO over SO<sub>2</sub>-pretreated Fe<sub>2</sub>O<sub>3</sub>/SiO<sub>2</sub> was oxidized by H<sub>2</sub>O<sub>2</sub>. The systematic research revealed that the generation of •OH from H<sub>2</sub>O<sub>2</sub> decomposition over adsorbed H<sub>2</sub>SO<sub>4</sub> was faster than that over Fe<sub>2</sub>O<sub>3</sub>/SiO<sub>2</sub>.

- **Keywords:** NO oxidation; SO<sub>2</sub>; H<sub>2</sub>O<sub>2</sub> vapor; Fe<sub>2</sub>O<sub>3</sub>/SiO<sub>2</sub>; Kinetic study

**Muthumariappan Akilarasan, Selvarasu Maheshwaran, Shen-Ming Chen, Elayappan Tamilalagan, Munirah D. Albaqami, Reham Ghazi Alotabi, Rameshkumar Arumugam. *In-situ synthesis of bimetallic chalcogenide SrS/Bi<sub>2</sub>S<sub>3</sub> nanocomposites as an efficient electrocatalyst for the selective voltammetric sensing of maleic hydrazide herbicide. Pages 151-160.***

The two-dimensional metal chalcogenides (TMC) have been fascinated more interest in a wide range of electrochemical applications owing to their high conductivity and excellent catalytic performance. Herein, we report the electrochemical sensor based on the urchin-like structured bimetallic strontium sulfide and bismuth sulfide (SrS/Bi<sub>2</sub>S<sub>3</sub>) nanocomposites prepared by a simple hydrothermal method. For the first time, the prepared SrS/Bi<sub>2</sub>S<sub>3</sub> nanocomposites were used to sense the carcinogenic herbicide maleic hydrazide (MHZ) in food and water samples. Moreover, the analytical performance of SrS/Bi<sub>2</sub>S<sub>3</sub> modified screen-printed carbon electrode (SrS/Bi<sub>2</sub>S<sub>3</sub>/SPC electrode) shows excellent results with a wide range of (0.01–104 μM and 104–814 μM), and the detection limit of 1.8 nM towards the MHZ detection. Furthermore, the developed sensor expressed good selectivity, repeatability, stability, and reproducibility. Finally, the real sample analysis of the developed sensor was tested in the potatoes and river water samples, which shows the recoveries of 97.8–98.9% and 97.2–98.2%.

- **Keywords:** SrS/Bi<sub>2</sub>S<sub>3</sub> nanocomposites; Environmental analysis; Maleic hydrazide herbicide; Pesticide detection; Electrochemical sensor

**Zhengen Zhou, Baozhong Ma, Chengyan Wang, Yongqiang Chen, Ling Wang. *Separation and recovery of scandium from high pressure sulfuric acid leach liquor of limonitic laterite. Pages 161-172.***

Extraction of Sc from Sc-rich limonitic laterite without interfering with the main nickel-cobalt production circuit will significantly enhance the economic value of laterite. A process for separation and recovery of Sc from high pressure acid leach (HPAL) liquor of limonitic laterite was proposed in this paper. Based on the chemical composition of the leach liquor, precipitation thermodynamic analysis and experiments were conducted. The results indicated that after a first step to precipitate Fe<sup>3+</sup> at pH = 2.5 and 90 °C, Sc could be enriched through a second step precipitate at pH = 4.8 and 60 °C to 267 g/t in Sc-containing precipitate. Then, Sc was re-leached from the Sc-containing precipitate via 1 mol/L sulfuric acid at L:S ratio of 5 mL/g, 80 °C, and 40 min. Meanwhile, gypsum in the Sc-containing precipitate transformed into calcium sulfate hemihydrate during leaching. After that, Sc was synergistically extracted from the leach solution via 5% P204 and 2.5% TBP. Moreover, impurities extracted into the organic phase during the extraction of Sc were scrubbed by HCl. Finally, Sc was stripped by NaOH. By using this process, Sc could be efficiently recovered from limonitic laterite in a facile way.

- **Keywords:** Limonitic laterite; Separation and recovery; Solvent extraction; Scandium

**Xudong Zheng, Biao Ji, Rong Jiang, Yawen Cui, Tongtong Xu, Man Zhou, Zhongyu Li. *Polydimethylsiloxane/carbonized bacterial cellulose sponge for oil/water separation*. Pages 173-180.**

Frequent oil spills from ships at sea have caused irreversible damage to the Marine environment. It is particularly important to develop environmentally friendly sorbent materials with special wettability and recyclability for oil/water separation. The polydimethylsiloxane/carbonized bacterial cellulose sponge (PDMS/CBC sponge) is self-assembled with PDMS as the matrix skeleton and CBC as the surface filler. With adding CBC, the elasticity and hydrophobicity of the PDMS composite sponge have been significantly improved. The PDMS/CBC sponge can be compressed to 80% deformation with only 1.45 MPa of force, and introducing of CBC makes the PDMS/CBC sponge more flexible. Even after 50 times of pressing, it can restore its original appearance and keep the internal channels from collapsing. The water contact angle of the PDMS/CBC sponge can reach 146.8°. The micro-nano structure substance CBC added into the surface of the low surface energy substance increases the roughness of the sponge and makes the sponge more lipophilic, which also makes the PDMS/CBC sponge have an excellent sorption ability of oil. And the sorption capacity of organic solvent/oil is from 300% to 900%. This super elasticity also allows material and regenerate by simple squeezing, and the sorption efficiency can reach 99.3% of the first time after 30 recycles. In addition, the PDMS/CBC sponge also shows a good sorption effect in an acid-base salt environment.

- **Keywords:** Polydimethylsiloxane; Carbonized bacterial cellulose; Hydrophobic; Elasticity; Oil/water separation

**Haitao Bian, Juncheng Jiang, Zhichao Zhu, Zhan Dou, Botao Tang. *Design and implementation of an early-stage monitoring system for iron sulfides oxidation*. Pages 181-190.**

Sulfur corrosion is one of the significant concerns that could cause potential hazards in the petrochemical industry, and the traditional periodical inspection techniques are insufficient to support timely and reliable monitoring of iron sulfides oxidation. The emerging data-driven fault detection models and innovative sensing technologies provide new opportunities to process safety monitoring. This article proposed an integrated approach that employed fiber-optic distributed temperature sensing (FO-DTS) system, electrochemical gas sensors, embedded systems, and neural networks to detect the exotherm of early-stage iron sulfides oxidation in complex scenarios. Specifically, the sulfides oxidation exotherm is simulated using programmed electrical heating devices, and a software simulation is conducted to optimize the heating rods power selection; the exothermic chemical reaction is carried out with the oxidation of dimethyl sulfoxide (DSMO) by hydrogen peroxide (H<sub>2</sub>O<sub>2</sub>) in a simulated stainless-steel reactor. The continuous temperature data and its spatial distribution of the targeted reactor surface are generated by the DTS, and the SO<sub>2</sub> concentration is collected as an additional criterion. The edge computing gateway can handle the field data collection from different types of protocols and other auxiliary tasks. Furthermore, the performance of the field sensing system and the anomaly detection neural networks are tested. The result shows that the proposed method is able to distinguish the simulated iron sulfides oxidation exotherm from the chemical reaction exotherm with an acceptable accuracy rate. The details of the system components are also demonstrated as a reference for deploying similar sulfides oxidation monitoring tasks in practice.

- **Keywords:** Process safety; Sulfur corrosion; Fault detection; Machine learning



**Shaodong Zheng, Jinsong Zhao. *High-fidelity positive-unlabeled deep learning for semi-supervised fault detection of chemical processes.* Pages 191-204.**

With the rapid development of the modern chemical process industry, process monitoring techniques have been investigated to enhance the loss prevention capability. Fault detection which attempts to detect whether an abnormal condition has happened is an essential step of process monitoring. Supervised learning based fault detection methods usually are not feasible in practical industry situations, because their most important prerequisite that adequate data labels are accessible is extremely hard to meet. In real industrial situations, a common scenario is that a few normal state data are labeled while no fault state data are labeled, and this is a natural fit for the positive-unlabeled (PU) learning. In this work, a three-step high-fidelity PU (THPU) approach based on deep learning is proposed for semi-supervised fault detection of chemical processes. A self-training nearest neighbors (STNN) algorithm is designed in Step 1 to conservatively generate a small reliable positive dataset by extracting data from the unlabeled training dataset. A positive and negative data recognition (PNDR) algorithm is designed in Step 2 to augment the reliable positive dataset and generate a reliable negative dataset based on the remaining unlabeled dataset. A convolutional neural network is trained in Step 3 based on the above reliable datasets as the binary classifier for online fault detection. The benchmark simulated Tennessee Eastman process dataset and a real industrial hydro-cracking process dataset are utilized to illustrate the effectiveness and robustness of the proposed THPU approach. The experimental results demonstrate the superiority of the proposed approach compared to the other competing PU learning approaches and supervised fault detection models.

- **Keywords:** Fault detection; Semi-supervised; PU learning; Deep learning; The Tennessee Eastman process; Hydro-cracking process

**Bo Ye, Jun Lan, Zexi Nong, Chaoke Qin, Maoyou Ye, Jialin Liang, Jinjin Li, Jiawei Bi, Weibao Huang. *Efficiently combined technology of precipitation, bipolar membrane electrodialysis, and adsorption for salt-containing soil washing wastewater treatment.* Pages 205-216.**

Wastewater of that washing of soil that results in concentrations of inorganic salts, toxic metals, chelating agents, and refractory dissolved organic matter may threaten the surrounding environment. Simultaneously, the removal of contaminants and the recovery of resources from this wastewater remain challenging. This study investigated the probability of a novel combined treatment (chemical precipitation + bipolar membrane electrodialysis (BMED) + activated carbon (AC) adsorption) on salt-containing soil washing wastewater treatment. The results showed that the proposed combined treatment could achieve proficient removal of heavy metals, inorganic salts, and total organic carbon (TOC) with low energy consumption (removal efficiency of heavy metals and inorganic salts > 94%; TOC removal > 58%). Meanwhile, the efficient recovery of acid and alkali could also be realized in the proposed treatment (acid-production rate =  $7.76 \pm 0.38$  mmol/h and base-production rate =  $5.47 \pm 0.42$  mmol/h at 50 mA/cm<sup>2</sup>). The mechanism result indicated that the chemical precipitation process could achieve high removal of heavy metals. Then, the BMED process induced an efficient separation of organic matter and inorganic salts. Accordingly, the AC adsorption process could efficiently remove organics. Preliminary economic evaluation results revealed that the combined process could proficiently treat the soil washing wastewater with economic viability. Together, these findings provide meaningful information for soil washing wastewater treatment with resource recovery.

- **Keywords:** Soil washing wastewater; Bipolar membrane electrodialysis; Activated carbon adsorption; Desalination; Wastewater recycling

**Hongqiu Zhu, Qiling Wang, Fengxue Zhang, Chunhua Yang, Yonggang Li, Can Zhou. Fuzzy comprehensive evaluation strategy for operating state of electrocoagulation purification process based on sliding window. Pages 217-229.**

In the process of electrocoagulation purification, there is a problem of passivation of the reactor electrode plates, and the process operating state is constantly changing, which badly affects the efficiency of electrocoagulation purification and the removal of heavy metal ion. However, in order to ensure that the concentration of heavy metal ion at the electrocoagulation outlet reaches the standard, the operators often replace the plates in advance or turn up the voltage to the maximum, resulting in increased power consumption and plates consumption. In order to solve this problem, this paper proposes a fuzzy comprehensive evaluation strategy for operating state of electrocoagulation purification process based on sliding window. Firstly, based on the combination of the Long and Short-Term Memory (LSTM) network and Autoregressive Integrated Moving Average Model (ARIMA), the predicted value of the removal rate of heavy metal ion in the electrocoagulation purification process is obtained. The predicted value and other important factors influencing the purification effect are used as the operating state evaluation indicators of the electrocoagulation purification process, and the operating state evaluation grade is divided according to the fuzzy rules. Secondly, the boxplot method is used to determine the threshold of each evaluation indicator, and the average value of the data of each indicator in each time window is calculated in real-time based on the sliding window. The current deterioration degree of each evaluation indicator is determined by the average value and the indicator threshold. Then, the basic weight of each evaluation indicator is calculated based on the grey relational analysis method, and the final weight of each indicator is determined according to the variable weight theory combined with the deterioration degree of each indicator. Finally, according to the fuzzy theory, the fuzzy comprehensive evaluation matrix is constructed by establishing the membership function, so as to evaluate the operating state of the electrocoagulation purification process. The effectiveness of the proposed evaluation strategy is verified by the industrial data collected from a wastewater treatment plant.

- **Keywords:** Electrocoagulation; Sliding window; Operating state; Fuzzy comprehensive evaluation

**Xuyan Liu, Hong Yang, Jiang Chang, Yongsheng Bai, Luyuan Shi, Bojun Su, Jun Han, Duo Liang. *Re-hydrolysis characteristics of alkaline fermentation liquid from waste activated sludge: Feasibility as a carbon source for nitrogen removal.* Pages 230-240.**

To overcome the issue of substandard nitrogen and phosphorus discharge, resulting from the low carbon/nitrogen (C/N) ratio of municipal wastewater, immobilized filler was used to re-hydrolyze the alkaline fermentation liquid of waste activate sludge (WAS) as a nitrogen removing carbon source. The complex organic matter was further hydrolyzed and its denitrification efficiency as a carbon source for nitrogen removal was improved. Volatile fatty acids increased from  $1605 \pm 5$  mg/L to  $2546 \pm 37$  mg/L after re-hydrolysis of mixed-alkali sludge fermentation liquid, and complex organic matter, such as fulvic acids, humic acids, class I aromatic proteins, and soluble microbial products were hydrolyzed into small-molecule organics. When the re-hydrolysis fermentation liquid (RH-SFL) was used as the carbon source for nitrogen removal, the nitrogen removal effect was close to sodium acetate and the nitrogen removal rate (NRR) was up to  $98.5 \pm 0.5\%$ . According to the NOX--N removal curve, the reaction rate of RH-SFL was significantly higher than before re-hydrolysis (nRH-SFL) ( $0.486 > 0.38$ ). This technology can significantly improve the effective organic quality in the alkaline fermentation liquid of WAS, which can be more easily utilized by denitrifying bacteria. This provides a

feasible and effective solution for nitrogen removal in municipal wastewater with insufficient carbon.

- **Keywords:** Waste activated sludge; Immobilized fillers; Re-hydrolysis; Carbon source; Denitrification

**Peyvand Valeh-e-Sheyda, Shokouh Sarlak, Forough Karimi. *Promoted alkanolamine solutions with amino acid L-arginine for post-combustion CO<sub>2</sub> capture in a micro-reactor. Pages 241-254.***

With the aim of replacing amine solvents, in the current study, the novel mixture solutions were proposed for CO<sub>2</sub> absorption combining amino acid (L-Arginine) with primary, secondary, and tertiary alkanolamines. The mass transfer performance of CO<sub>2</sub> capture in the aqueous solutions of MEA-ARG, DEA-ARG, and MDEA-ARG was intensified under operational conditions of 4–12 wt% arginine concentration, 120–300 mL/min feed solvent flow rate, 3–9 mL/min inlet gas flow rate. In this regard, a T-shape micro-reactor with a diameter of 800  $\mu$  and a length of 29.5 cm was utilized. All the experiments were performed under the atmospheric pressure and absorption temperature of 45 °C. Considering industrial restrictions, the total concentration of mixtures was kept constant at 25 wt% for MEA-ARG, 35 wt% for DEA-ARG, and 50 wt% for MDEA-ARG. The results of CO<sub>2</sub> absorption efficiency (ef), overall volumetric mass transfer coefficient, OVGMTc, (KGaV), and volumetric mass transfer flux (NAaV) indicated that in all three cases, the aqueous MEA-ARG solution has the highest value of 96%, 90.95 kmol/m<sup>3</sup>.h.kPa, and 361.82 kmol/h.m<sup>3</sup>, respectively. Also, while the gas and liquid flow rates were kept constant in their middle points, adding arginine from 4 to 12 wt% enhanced the values of the ef from 92.55% to 93.76% for DEA-ARG and from 79.20% to 93.23% for MDEA-ARG solutions, respectively. However, the results were obtained differently for solution MEA-ARG.

- **Keywords:** Absorption; Alkanolamine; Carbon dioxide; Micro-reactor; L-Arginine; Overall volumetric gas-phase mass transfer coefficient

**Peng Yang, Rongrong Hou, Rongfang Yuan, Fei Wang, Zhongbing Chen, Beihai Zhou, Huilun Chen. *Effect of intermittent operation and shunt wastewater on pollutant removal and microbial community changes in subsurface wastewater infiltration system. Pages 255-265.***

Subsurface wastewater infiltration system (SWIS) is widely used in the treatment of rural domestic sewage. However, the nitrogen removal effect is unsatisfactory. In this study, laboratory-scale SWIS was built, and the nitrogen removal capacity of the system was optimized by a combination of intermittent operation and the shunt method. The optimal total nitrogen (TN) removal rate (56.53%) is obtained when the wet-dry ratio (Rwd) is 1:2 and the shunt ratio is 3:1. The optimal ammonia nitrogen (NH<sub>4</sub><sup>+</sup>-N) removal rate (54.97%) is obtained when Rwd is 1:3 and shunt ratio is 2:1. In addition, SWIS achieved a good COD removal rate (>75%) and TP removal rate (>95%) during the whole operation stage. Proteobacteria, Acidobacteria and Bacteroidetes are high abundance phyla in SWIS. Bacteroidetes, Chloroflexi and Nitrospirae associated with nitrogen removal are abundant at the shunt ratio of 2:1 and 3:1. At the genus level, Bosea, Bradyrhizobium and Phenylobacterium were functional genera associated with denitrification, enriching the substratum of SWIS at shunt ratios of 1:1, 2:1 and 3:1. Nitrogen (N) forms and ORP analysis showed that under the appropriate shunt ratio and Rwd, the SWIS matrix has a suitable redox microenvironment, and thus creates a well-defined nitrification area and denitrification area. This research provides a reliable theoretical basis for the construction and operation of SWIS in rural areas.

- **Keywords:** Subsurface wastewater infiltration system; Pollutant removal; Microbial community; Intermittent operation; Shunt wastewater

**Yanchao Shi, Ning Wang, Jian Cui, Changhui Li, Xuejie Zhang. *Experimental and numerical investigation of charge shape effect on blast load induced by near-field explosions*. Pages 266-277.**

High explosives are hazardous materials that are frequently used in industrial production which involves many safety and risk problems. To investigate the influence of the explosive charge shape on near-field blast loads ( $<1.0 \text{ m/kg}^{1/3}$  in this study), 12 shots of field blast tests were carried out. The reflected overpressures of 1 kg TNT with different charge shapes at a distance of 800 mm and the incident overpressures at a distance of 1310 mm were measured and analyzed. The fireballs produced by the explosions were recorded by a high-speed camera and compared with each other. Results show that the fireball of a non-spatial symmetry explosive is non-uniformly distributed, which indicates the released energy is also non-uniform. The charge shape effect was further investigated using a verified numerical model. The experimental and numerical results show that the charge shape has a significant effect on the key parameters of blast loads such as the incident overpressure, the reflected overpressure, and the impulse. However, the influence of the charge shapes crumbled away with the increase of scaled distance. When the scaled distance is larger than 5.0 (6.0)  $\text{m/kg}^{1/3}$ , the hemispherical (cylindrical) charge shape effect on the reflected peak overpressure and the impulse can be neglected.

- **Keywords:** Blast loads; Charge shape; Reflected overpressure; Blast-resistant design; Field blast tests

**Kui Huang, Hao Xiong, Haili Dong, Yuling Liu, Yuanhuan Lu, Kunjie Liu, Junzhen Wang. *Carbon thermal reduction of waste ternary cathode materials and wet magnetic separation based on Ni/MnO nanocomposite particles*. Pages 278-285.**

The widespread use of lithium-ion batteries and the increase in the number of new energy electric vehicles have brought more waste batteries to be recycled. In this paper, a new combined process for in-situ recycling of wasted ternary lithium batteries using graphite for carbon thermal reduction with the cathode material under nitrogen atmosphere, after which the nanocomposite particles formed by the reduction products were separated and recovered by wet magnetic separation, has been proposed. The carbon thermal reduction products were  $\text{Li}_2\text{CO}_3$ , Ni, Co and MnO, respectively, and Ni and Co could form nanocomposite particles with MnO in the thermal reduction process. The reaction mechanism of the carbon thermal reduction reaction of anode materials and the effects of carbon thermal reduction temperature, wet magnetic separation time and solid-to-liquid ratio on the recovery rate were investigated. The recovery rate of Li, Ni, Co and Mn were 95.57 %, 96.44 %, 94.88 % and 94.98 %, respectively, under the optimum condition of reaction temperature of 650 °C, wet magnetic separation time of 75 min and solid-liquid ratio of 15 g/L, respectively.

- **Keywords:** Ternary lithium batteries; Pyrometallurgy; Wet magnetic separation; Nanocomposite particles

**Huaming Da, Hepeng Yin, Guangqian Liang. *Explosion inhibition of coal dust clouds under coal gasification atmosphere by talc powder*. Pages 286-294.**

During coal gasification, the explosion intensity of coal dust was enhanced and more difficult to inhibit due to the presence of CO and H<sub>2</sub>. To mitigate the risk of dust explosion under a coal gasification atmosphere, the inhibition performance of talc powder (TP) on coal dust explosion was investigated by using a 20 L spherical explosive vessel. The results showed that the explosion intensity of dust clouds was attenuated with the

inhibition of TP. As the particle size of TP decreased, the explosion pressure gradually was reduced and the explosion time was extended. The maximum explosion pressure of dust clouds decreased from 0.845 to 0.270 MPa after the addition of 8000 mesh TP, representing a reduction of 68 %. And the flame propagation velocity was consequently dropped from 1.22 to 0.17 m/s. Moreover, the explosion of higher rank coal dust was more easily inhibited by TP. XPS analysis demonstrated that the C–C and C–O–C in coal dust were effectively protected under the effect of TP. And the inhibition mechanism of TP on coal dust explosion was elaborated thoroughly in combination with the analysis of explosion products.

- **Keywords:** Coal gasification; Coal dust explosion; Talc powder; Explosion inhibition

**Huajie Wang, Feng Qiu, Hongliang Qian, Huili Hu, Yu Gao, Shijin Chen, Feng Fan. *Integrated analysis method of 3D corrosion evolution and mechanics of steel based on electrochemical corrosion mechanism. Pages 295-306.***

As the primary raw material of steel structure buildings, steel is sensitive to environmental factors and prone to electrochemical corrosion, which poses a serious threat to the safety of the whole structure. The mechanical property degradation of steel structures after corrosion is not only related to the corrosion depth but also closely related to the uneven corrosion morphology and location distribution in 3D space. Based on this, this paper proposed an integrated method that can realize the 3D corrosion evolution prediction process on steel member surface and the evaluation of its mechanical properties respectively. Through the method, the real-time dynamic changes of 3D corrosion interface can be tracked based on electrochemical corrosion mechanism and level-set model. Then the results of corrosion evolution can be conveniently converted into mechanical analysis models for loading solution. The prediction effect and mechanical analysis function of the method were verified by a salt spray exposure corrosion test of Q235 steel and a compression loading test of a long-term corroded steel plate. The integrated method can provide a method support for predicting the remaining service life of steel structures in corrosive environments, reasonably selecting maintenance time and preventing collapse in the future.

- **Keywords:** Steel materials; Electrochemical corrosion; Level-set model; 3D evolution; Corrosion morphology

**Alireza Ebrahimi, Mohammad Haghghi, Sogand Aghamohammadi. *Sono-precipitation fabrication of ZnO over modified SAPO-34 zeotype for effective degradation of methylene blue pollutant under simulated solar light illumination. Pages 307-322.***

Implementation of hierarchical SAPO-34 zeotype, which was synthesized via a hard-template technique using secondary hard template, as a photocatalyst support for ZnO photocatalyst has been investigated. The ZnO/SAPO-34 (AC-U)-U photocatalyst was applied for photodegradation of dye molecules under simulated-solar-light irradiation. X-ray diffraction (XRD), field-emission scanning-electron-microscope (FESEM), Barrett-Joyner-Halenda (BET-BJH), Differential reflectance spectroscopy (DRS), Temperature-programmed reduction of hydrogen (H<sub>2</sub>-TPR) and Photoluminescence spectroscopy (PL) analyses have been applied to investigate the physiochemical properties of the catalysts. The BET-BJH results indicated that applying hard-template (active carbon) coupled with sonication leads to a raise in mean pore diameter of sample from 0.5 to 16.6 nm (about 32 folds higher). H<sub>2</sub>-TPR analysis confirms that the ZnO is dispersed uniformly by utilizing sonication. Furthermore, morphological analyses showed that the sonicated sample have more channel-like defect on the surface. PL analysis demonstrates the lower

recombination rate of electrons-holes for the composite structure. The hierarchical architecture compared to the conventional pore structure has significantly increased adsorption capacity of dye from 10.8% to 50.3% by modifying the texture and pore structure. Sonicated photocatalyst showed the highest methylene blue degradation efficiency (95.7%). Hence, the ZnO/SAPO-34 (AC-U)-U nanocomposite photocatalyst depicts as a promising reusable photocatalyst for the photodegradation of dye-polluted water.

- **Keywords:** Pore-engineered zeotype; ZnO/SAPO-34; Photocatalytic degradation; Dye pollutant; Water treatment

**Sai Zhang, Ruoning Guo, Ming Liang, Li Li. *Regulation of ZnFe<sub>2</sub>O<sub>4</sub> synthesis for optimizing photoelectric response and its application for ciprofloxacin degradation: The synergistic effect with peroxymonosulfate and visible light.* Pages 323-335.**

ZnFe<sub>2</sub>O<sub>4</sub> (ZFO) poses great potential to activate peroxymonosulfate (PMS) and responds to visible light. In this work, ZFO was synthesized by a simple one-step hydrothermal method. In order to obtain the most desirable photoelectric performance, hydrothermal reaction parameters including pH, temperature, and time were innovatively regulated. Based on optimized ZFO, the visible light/PMS/ZFO (Vis/PMS/ZFO) system was established, which presented superior degradation efficiency of ciprofloxacin (CIP). It was verified that •OH and  $^{1}O_2$  were the main reactive species for CIP degradation. Besides, visible light was confirmed to promote formation of reactive species and accelerate charge transfer simultaneously. Therefore, the possible mechanism of catalysis was proposed and the enhancement of visible light for the PMS/ZFO system was elaborated. Based on the identified intermediates, three pathways of CIP degradation were illustrated. Moreover, water matrix posed an overall positive impact on CIP degradation. Experiments performing in real wastewater and repeated tests validated wide application of the Vis/PMS/ZFO system. In general, the designed synthesis of ZFO is feasible and the integration of ZFO with visible light for efficient PMS activation is a successful and promising method for wastewater treatment.

- **Keywords:** ZnFe<sub>2</sub>O<sub>4</sub>; Peroxymonosulfate; Ciprofloxacin; Visible light; Heterogeneous catalysis

**Youlong Chen, Zhenming Sun, Yunbing Hou, Dong Gao, Zhongxue Li. *Hazard identification & risk control in aluminum production.* Pages 336-346.**

With the rapid development of China's economy, the safe production of electrolytic aluminum is becoming increasingly prominent. It is particularly important for the production safety of the electrolytic aluminum industry to identify the hazards of electrolytic aluminum operation and find a practical and effective operational risk control method. A two-dimension hazard classification method and an evidence - based hazard identification framework are put forward. A process oriented hazard evolution and risk control method system is constructed, which provides a theoretical method for systematically investigating hazards, reducing risks and preventing and controlling accidents. Taking the molten aluminum explosion accident in an electrolytic workshop section as an example, the hazards were identified, the process from hazards to accident was analyzed by means of a fault tree, event tree and bow tie diagram, and a hazard evolution path was selected to set up safety measures to explain the feasibility of risk control methods.

- **Keywords:** Molten aluminum; Hazard identification; Risk control; Explosion accident

**Shanlong Tao, Yong Zhu, Chen Chen, Jiahua Liu, Mingxia Chen, Wenfeng Shangguan. *Removal of air pollutant by a spike-tubular electrostatic device: Multi-stage direct current corona discharge enhanced electrostatic precipitation and oxidation ability.* Pages 347-356.**

In this work, a spike-tubular electrostatic device was developed for effectively removing particulate matter (PM) and VOCs, based on multi-stage electric field enhancement and expanded arc interface ratio of corona discharge. In the experiment, it was equipped with a portable 12 V D.C. power supply module and a fan module; PM from moxa smoke, mainly composed of submicron particles with a high penetrate rate, and HCHO were employed to test its electrostatic precipitation and oxidation ability, respectively. Additionally, CFD numerical simulation was adopted to investigate the characteristics of the electric field, the flow field, and the ozone generation. Experimental results showed that the electrostatic device could remove 99% of the fine particles at 2 m/s. Meanwhile, it could also remove HCHO of  $2.14 \times 10^3$ - $1.07 \times 10^4$   $\mu\text{g}/\text{m}^3$  concentration with 100% efficiency. By comparison, its oxidation capacity could be about 80 times that of ozone oxidation, revealing the enhanced oxidation ability of other short-living reactive species. Simulation results proved that the promising purification performance resulted from the locally enhanced electric field strength, up to  $2 \times 10^7$  V/m in the central region, and sufficient contact between pollutants and the corona discharge region. Finally, as verified by the airtight chamber cycle experiment and case comparison, the device owns feasible purification ability and promising energy yield (0.79 g/kWh) in the application. Moreover, prospects and strategies for the device's practical application in air purification and disinfection were proposed, which may provide helpful enlightenment for air purification.

- **Keywords:** Spike-tubular; Multi-stage electric field; Corona discharge; Particle; Oxidation; Numerical simulation

**Heloísa Bremm Madalosso, Bianca de Castro Santos, Luiz Fernando Belchior Ribeiro, Ricardo Antonio Francisco Machado, Cintia Marangoni. *Improvement of membrane hydrophobicity by one-step electro spraying for water recovery from textile dye solutions by membrane distillation.* Pages 357-373.**

Membrane distillation is an upcoming technology for water recovery from industrial effluents. However, inherent operational phenomena, such as membrane wetting, compromise its functioning with complex solutions. Membrane modification can be a key to mitigating membrane gaps. Herein, a polypropylene membrane was physically modified via one-step electro spraying using a polymeric blend of polydimethylsiloxane and polyvinylidene fluoride. The main goal was to improve membrane hydrophobicity and enhance DCMD performance with four dye classes (Reactive, Disperse, Direct, and Acid). Polymer reticulation and polymer concentration in dope solution were studied, affecting membrane hydrophobicity. The modification improved the water contact angle by 20% after 90 min under the spray containing 2% PVDF and 6% PDMS-cured. The modified PP membrane reached contact angles of  $148.38 \pm 2.36^\circ$  and  $151.5 \pm 6.18^\circ$  for direct and acid dyes, respectively. The modified layer increased the membrane thickness by 3  $\mu\text{m}$  without significant porosity alterations, amplifying the pH range where membranes assume negative charges. Stable permeate fluxes on a DCMD operation were reached, varying between 29.7 and 44.85  $\text{L m}^{-2} \text{h}^{-1}$ , and the rejection rate increased to 6%. The modification enhanced the membrane performance with textile dye solutions, enabling MD operation to water reclamation from textile effluents.

- **Keywords:** Membrane modification; PDMS; PP; PVDF; DCMD; Reactive dye; Textile wastewater

**Yuvarajan Devarajan, Ravikumar Jayabal, Dinesh Babu Munuswamy, S. Ganesan, Edwin Geo Varuvel. *Biofuel from leather waste fat to lower diesel engine emissions: Valuable solution for lowering fossil fuel usage and perception on waste management.* Pages 374-379.**

This work examines the viability of examining waste fat extracted from industrial leather waste as an alternative to diesel. These wastes are harmful if disposed to the environment. Conventional transesterification was performed to produce leather waste methyl ester (LWME). Post-processing, a yield of 82.6% of methyl ester was obtained. The obtained LWME was inspected for its thermophysical properties and falls with ASTM standards. LWME was blended with petroleum diesel at 10%, 20% and 30% on a volume basis and referred to as LWME10D90, LWME20D80 and LWME30D70 correspondingly. The effect of LWME/ diesel blends was inspected in a four-stroke, single-cylinder, direct-injection engine under diverse loads. Test results revealed that the brake thermal efficiency for LWME/ diesel blends was lower than diesel at all loads with higher specific brake-specific fuel consumption was higher as both are inversely proportional. Carbon monoxide emissions were reduced by 22.7%, Hydrocarbon emissions were reduced by 48%, and Smoke emissions were reduced by 6.43%, with a 9.84% increase in nitrogen oxide emissions for LWME30D70 than diesel. It has been concluded that including LWME in diesel lowers the greenhouse gases with a marginal reduction in performance pattern.

- **Keywords:** Methyl ester; Engine performance; Tailpipe emissions; Waste to energy; Diesel engine

**Xianlian Wang, Qingsong Hua, Ping Liu, Li Sun. *Stochastic dynamic programming based optimal energy scheduling for a hybrid fuel cell/PV/battery system under uncertainty.* Pages 380-386.**

Hybrid green energy system, consisting of photovoltaic (PV), fuel cell and battery, receives wide attention because of its autonomy, flexibility and promising potential in accelerating the development of carbon neutrality in the field of power generation. However, the efficient power dispatching of the hybrid energy system is challenging due to the inevitable uncertainties of the solar energy. To this end, stochastic dynamic programming (SDP) is used in this paper to find the optimal solution to minimize the total fuel consumption during a 72-hour operating cycle, with constraints on the magnitude and rate of the fuel cell and battery operation, in which the stochastic characteristics of the solar power are described by Markov chain. The influence of sampling time and number of states on the solar prediction accuracy is discussed. For comparison, the traditional rule-based algorithm and dynamic programming (DP) algorithms are also utilized to describe and solve the power distribution problem, corresponding to different decision results in terms of how to distribute the energy flow for each time period. Numerical optimization results within the 72-hour period demonstrate that, the SDP has a 20.61% economy and 66.34% battery SOC improvement than that of rule-based algorithm, and in most uncertain cases, the SDP produces superior economic performance than those of both the rule-based algorithm and DP, benefited from the inclusion of the solar power probabilities into the optimization framework. The results of this paper lay a solid foundation for the efficient energy management of the hydrogen and solar hybrid energy system.

- **Keywords:** Energy management; Markov chain; Stochastic dynamic programming; Hybrid energy system



**Yifan Wang, Xing Zheng, Dongfei Li, Fangang Meng, Jiayu Tian, Mian Wang, Li Li, Hua Wu, Yaozhong Zhang. *Effect of sodium and potassium on polysaccharide fouling on PVDF and graphene oxide modified PVDF membrane surfaces. Pages 387-395.***

This study presented the contribution of monovalent cations (Na<sup>+</sup> and K<sup>+</sup>) to the adsorptive sodium alginate (SA) fouling in real-time using a quartz crystal microbalance and dissipation (QCM-D). Polyvinylidene fluoride (PVDF) and graphene oxide modified PVDF membrane (GO-PVDF) were selected as representative membrane materials. Atomic force microscopic (AFM) equipped with probes modified with foulant was used for exploring the adhesion force changes between SA and the membrane. The results showed that both Na<sup>+</sup> and K<sup>+</sup> can promote the adsorption capacity of SA on the membrane surface. SA fouling in Na<sup>+</sup> condition was more severe than that in K<sup>+</sup> circumstance due to higher attraction forces under identical ion strength. In addition, the GO-PVDF membrane is more readily/severely fouled than PVDF by SA when Na<sup>+</sup> or K<sup>+</sup> is present. The difference in the interaction forces was further interpreted using XDLVO theory. The results suggested that the Lewis acid-base adhesion free energy ( $\Delta G_{\text{LFB}}$ ) between SA decreased gradually with increasing Na<sup>+</sup> concentration, while in the K<sup>+</sup> environment,  $\Delta G_{\text{LFB}}$  increased instead. Moreover, the increase of the Lifshitz-van der Waals components ( $\gamma_{\text{mLW}}$ ) of the GO membrane, resulted in a higher attractive interaction in the initial phase of the SA fouling. The results of this study provide a microscopic analysis of the possible fouling mechanism of Na<sup>+</sup> and K<sup>+</sup> on membrane fouling and as well as provide insightful reflections for an appropriate approach (whether GO modified or not) to membrane fouling control.

- **Keywords:** Monovalent cation; Polysaccharide; GO-PVDF membrane; Membrane fouling

**Sam Slatnick, D. Angevine, J. Cranefield, C. Maddox, M. Overstake, L. Palmer, A. Younan. *Bow-ties use for high-consequence marine risks of offshore structures. Pages 396-407.***

Bow-ties are used in multiple industries to effectively manage safeguards during operation. Benefits of bow-ties include clear communication, operator ownership, relationship between safeguards for various threats and consequences, and the visibility of safeguard health during operations. In oil and gas, the main application of bow-ties has been to manage high consequence risks pertaining to process safety, i.e. loss of primary containment of hazardous substances. Offshore structural and marine failures are not always driven by loss of primary containment, and as a result the use of bow-ties in offshore structures and marine is less established. This paper expands the application of process safety bow-ties into failure risks for structural and marine offshore facilities. First it's introduced as a general framework, then implemented to select high-consequence offshore facility scenarios. Though less conventional than common approaches for designing against structural and marine failure scenarios, use of bow-ties is distinguished in its ability to manage risks which are mitigated by operational safeguards, such as ice feature overloads, offshore collisions, multi-line mooring failures, and loss of floating stability.

- **Keywords:** Bow-tie analysis; Facility; Failure; Fatality; Hazard; Marine; Mitigation; Offshore; Oil and gas; Process safety; Risk scenario

**Bo Lv, Feishuo Jiao, Zengqiang Chen, Bobing Dong, Chaojun Fang, Chuanxiang Zhang, Xiaowei Deng. *Separation of unburned carbon from coal fly ash: Pre-classification in liquid–solid fluidized beds and subsequent flotation*. Pages 408-419.**

Coal fly ash, which is the solid waste produced during the coal combustion and utilization, causes serious environmental problems. The preparation of concrete from coal fly ash has been proven helpful in potentially improving its value and reducing its environmental impact to a certain extent. However, the presence of unburned carbon components affects the performance of coal fly ash-based concrete. In this study, unburned carbon is separated from coal fly ash by pre-classification and subsequent optimized flotation, wherein the factors influencing are explored. The results show that under the pre-classification function of the inflatable-inclined liquid–solid fluidized bed, the underflow product is enriched in unburned carbon particles, with loss-on-ignition (LOI) and yield ( $Y_o$ ) values of 11.58 % and 72.87 %, respectively. Further, the underflow product is floated for a cleaner carbon product, which is affected by the stirring rate ( $W$ ) and the amount of collecting agent ( $C$ ) and foaming agent ( $F_o$ ). Optimized flotation (i.e.,  $C = 18$  kg/t,  $F_o = 6.5$  kg/t,  $W = 1600$  rad/min) results in the maximum combustible recovery rate of the flotation concentrate (89.89%), with LOI of 41.80 % and  $Y_o$  of 18.51 %, yielding unburned carbon products for fuel. After mixing the flotation tailings with the pre-classified overflow production, the LOI of the formed ash-rich product is 1.73% with  $Y_o$  of 81.49%, prepared into concrete. Thus, the proposed pre-classification and flotation process can improve the quality of coal fly ash. The results provide a theoretical basis for the harmless and resource treatment of coal fly ash.

- **Keywords:** Coal fly ash; Inflatable-inclined liquid–solid fluidized bed; Pre-classification process; Ash product; Optimized flotation

**Jonghun Lim, Yuchan Ahn, Hyungtae Cho, Junghwan Kim. *Optimal strategy to sort plastic waste considering economic feasibility to increase recycling efficiency*. Pages 420-430.**

In this study, we suggested an optimal strategy to sort plastic waste to improve recycling efficiency considering economic feasibility. To derive the optimal sorting strategy, we developed a novel optimization model that considers the overall cost, which is sorting cost minus the revenue obtained by selling the recycling plastic from the sorting cost. Then we used the developed model to identify the optimal strategy to sort plastic waste in mixed-integer programming that minimizes the overall cost of plastic waste sorting systems. We also conducted a sensitivity analysis to analyze the extent to which the results obtained can change under different conditions. The optimization results, identify that the plastics in the optimal sorting strategy are of four types: LDPE, HDPE, PP, and PVC. This optimal sorting strategy increase the overall sorting efficiency slightly by 4 wt%, but considering the revenue obtained by selling the recycled plastic the strategy significantly decreased the overall sorting cost by 69.28 % compared to the conventional case. The developed model can determine the optimal strategy to sort plastic waste considering economic improvement. Therefore, the results allow increase in plastic recycling by minimizing the overall cost of the sorting system.

- **Keywords:** Plastic waste; Sorting; Recycling efficiency; Optimization

**Anum Nosheen, Muhammad Tahir Hussain, Madiha Khalid, Amjed Javid, Humera Aziz, Shazia Iqbal, Munir Ashraf, Sultan Ali. *Development of protective cotton textiles against biohazards and harmful UV radiation using eco-friendly novel fiber-reactive bioactive agent. Pages 431-444.***

Due to the increase in biological hazards to global security particularly after COVID-19 crises, the need to develop effective and adaptable technologies to protect humans from biological warfare agents (viruses, bacteria, fungi) has increased. Current protective textiles against biohazards are fabricated through finishing of textiles with bioactive agents. However, bioactive agents are leached from the treated textiles due to the poor durability following their accumulation in environment. The objective of this research was to design a sustainable approach for developing ecologically sound antimicrobial textiles in which the antimicrobial agent is covalently bonded to fabric and does not leach into the effluent when laundered. For this, a novel bifunctional reactive finish was synthesized in which chloroxylenol (antimicrobial agent) was covalently integrated into two reactive systems (triazine and vinyl sulfone). For structural validation, <sup>13</sup>C NMR, <sup>1</sup>H NMR, and FTIR characterization were employed. The as-synthesized reactive finish was applied on the cotton fabric through pad-dry-cure method. The antimicrobial action of treated fabric (before and after 20 laundry cycles) towards viruses, bacteria, and fungi as well as ultraviolet protection factor (UPF) were evaluated according to standard. The treated fabric showed significant fungicidal (>85 %) bactericidal (>95 %), and viricidal (>85 %) action, that remained effective even after 20 washes, revealing that antimicrobial agent has not leached during washing of treated textiles which established non-leaching behavior of the treated textiles. The treated fabric also exhibited outstanding UPF values (>135). The current study has proposed a novel approach for the fabrication of ecologically sustainable antimicrobial textiles and the proposed method is easily scalable at industrial level.

- **Keywords:** Novel bifunctional finish; Non-leaching; Sustainable multifunctional textiles; Durability; Reusability; Mechanical properties, comfort properties

**Mingxue Xin, Yingjie Sun, Yinkai Wu, Weihua Li, Junquan Yin, Yuyang Long, Xuebin Wang, Ya-nan Wang, Yaomin Huang, Huawei Wang. *Stabilized MSW incineration fly ash co-landfilled with organic waste: Leaching pattern of heavy metals and related influencing factors. Pages 445-452.***

Toxicity Characteristic Leaching Procedure (TCLP, USA) and Acetic Acid Buffer Solution Method (HJ/T 300-2007, China) are often used to simulate the leaching process of heavy metals from MSW incineration fly ash after entering sanitary landfill under the influence of landfill leachate. However, the results based on the standards can neither obtain the actual leaching pattern of heavy metals, nor evaluate or predict their environmental risk evolution. In this study, the leachate characteristics and leachability of Cd, Cu, Pb, Zn, Cr, and Ni during the co-landfilling of chelating agents or phosphate stabilized fly ash and MSW were investigated using three simulated landfill columns under rainfall conditions. The maximum leaching concentration of Pb and Cd in the co-landfill of chelate stabilized fly ash and MSW exceeded the corresponding standard limits, and that of Pb, Cd, and Ni for the scenario of co-landfill of phosphate stabilized fly ash and MSW exceeded the corresponding standard limits. In general, there were higher leaching concentrations of heavy metals in the initial stage (Pb, Cd, Zn, and Cr) and middle stages (Cu and Ni) of the landfill. Compared with those of the landfill with MSW alone, the pH, volatile fatty acids (VFA) and ammonia (NH<sub>4</sub><sup>+</sup>-N) concentration were high in the leachate from the co-landfill with stabilized fly ash and MSW. The pH and chemical oxygen demand (COD) of the leachate might be the primary factors affecting the leaching behavior of heavy metals, whereas VFA and NH<sub>4</sub><sup>+</sup>-N seemed to have little effect. This study demonstrated

that evaluating the leaching risk of heavy metals according to actual disposal scenarios, is a more effective method than the standard methods.

- **Keywords:** Municipal solid waste (MSW); MSW incineration fly ash; Co-landfill; Heavy metal leaching; Rainfall

**Gang Zhou, Zhanyi Xing, Yichun Tian, Bingyou Jiang, Bo Ren, Xiaosu Dong, Longxiao Yi. *An environmental-friendly oil-based dust suppression microcapsules: Structure with chitosan derivative as capsule wall.* Pages 453-462.**

In this study, environmentally friendly microcapsules with chitosan quaternary ammonium salt (HACC) and sodium alginate (SA) shells and rapeseed oil cores were used to harmlessly reduce the dangers of open pit coal mine dust to coal miners. Due to the electrostatic attraction between  $-NH_3^+$  of HACC and  $-COOH^-$  of SA, the complex coacervation method was used to coat the rapeseed oil core material to prepare a type of oil-based dust suppression microcapsules. Optical and scanning electron microscopy showed that the microcapsules had a spherical structure, smooth surface without holes, core-shell structure, and sustained release properties. Infrared spectroscopy and X-ray diffraction showed that HACC and SA were electrostatically attracted to form a kind of "eggshell" structure-coated core material. Thermogravimetric analysis showed that the microencapsulated rapeseed oil had good thermal stability. Performance tests showed that rapeseed oil adheres well to the dust, the shell material and the dust form a strong solid layer, and the core and shell materials work synergistically to suppress coal dust. The dust suppression rate reached up to 91.98 %. In addition, the dust suppression microcapsules have good water retention performance and degradability, which can reduce the harm to the environment.

- **Keywords:** Open pit coal mine dust; Dust suppression microcapsules; Rapeseed oil; Complex coagulation; Biodegradation

**R. Rajesh Alias Harinarayan, S. Mercy Shalinie. *XFDDC: eXplainable Fault Detection Diagnosis and Correction framework for chemical process systems.* Pages 463-474.**

Industry 4.0 process fault detection and diagnosis(FDD) is built on the foundations of Industrial Internet of Things(IIoT) for sensing and artificial intelligence for recognizing patterns. Despite the performance and application of various learning-based algorithms in multiple sectors, their black-box nature makes industrial experts skeptical. So, this paper proposes an eXplainable Fault Detection, Diagnosis, and Correction(XFDDC) Framework to create best-fit FDD models that are explainable. The XFDDC framework is designed to explain the FDD model predictions using eXplainable Artificial Intelligence(XAI) techniques. The proposed framework was applied to the bench-marked Tennessee Eastman Process(TEP) dataset. On evaluation, an XGBoost model yielded better Fault Detection Rate(FDR) and F1 score against popular transparent and complex models like Naive Bayes, K-Nearest Neighbors, Random Forest and a rule-based version of XGBoost. To explain the predictions of the XGBoost model, the XFDDC framework suggests the use of feature-based XAI techniques. So, the TreeSHAP algorithm is applied on the XGBoost model to generate local and global explanations as part of fault diagnosis. The proposed framework also recommends counterfactual explanations to provide action recommendations for correcting the fault situation. Thus, a best-fit explainable XGBoost Fault Detection, Diagnosis, and Correction (XGBoost-XFDDC) model is created.

- **Keywords:** Chemical process; Process safety; Fault detection; Fault diagnosis; Explainable artificial intelligence; Fault correction

**Wenyuan Li, Chenyang Zhang, Xin Wei, Hongliang Zhang, Mingjun Han, Wei Sun, Wenzhang Li. *Efficient resource treatment of hexavalent chromium wastewater based on lead carbonate (cerussite)-induced precipitation separation. Pages 475-486.***

Recycling treatment of wastewater containing hexavalent chromium [Cr (VI)] has always been an important environmental issue. In this paper, taking advantage of the natural affinity of  $\text{CrO}_4^{2-}$  and lead ions, lead carbonate was selected as a precipitant to recover Cr (VI) in the form of chrome yellow ( $\text{PbCrO}_4$ ). Firstly, the variation of Cr (VI) and lead species in  $\text{K}^+-\text{CrO}_4^{2-}-\text{Pb}^{2+}-\text{CO}_3^{2-}$  solution system with pH and  $\text{PbCO}_3$  dosage was calculated by Visual MINTEQ. The results show that the treatment effect is better under acidic conditions. Then, the effects of parameters on the removal rate of Cr, including the initial pH of solution, reaction time, reaction temperature, and the dosage of lead carbonate, were studied by batch experiments. Results show that the initial pH of solution, reaction time, and the dosage of lead carbonate have great influence, whereas reaction temperature has slight influence. And the concentration of Cr (VI) could be reduced from 100 mg/L to 0.043 mg/L at an initial pH of 3, a reaction time of 45 min, and the dosage of lead carbonate as  $n(\text{PbCO}_3)/n(\text{K}_2\text{CrO}_4) = 2$ . The precipitates are analyzed by XRD, SEM, and EDS, and the results are consistent with the predictions of Visual MINTEQ, that is, the newly produced substance is only  $\text{PbCrO}_4$ . The reaction mechanism of Cr (VI) on the surface of lead carbonate was studied by the adsorption kinetic model, and the results showed that the reaction was more fit with the pseudo-second-order kinetic model. Density functional theory (DFT) calculations show that  $\text{CrO}_4^{2-}$  could effectively react with lead atoms with unsaturated coordination bonds on the surface of lead carbonate and free lead ions leached from the surface of lead carbonate to form lead chromate. Under acidic conditions, the removal of Cr (VI) by  $\text{PbCO}_3$  may involve two main mechanisms: the mineralization and precipitation of lead and chromate ions dissolved from the surface of cerussite and the chemical adsorption of chromate ions on the surface of cerussite. This study provides a new and efficient strategy for the resource treatment of Cr (VI)-containing wastewater.

- **Keywords:** Chromium (VI) wastewater; Precipitation; Lead Carbonate; Resource recycling; DFT

**Zhanwei He, Xiaojun Hu, Kuo-Chih Chou. *Synergetic modification of industrial basic oxygen furnace slag and copper slag for efficient iron recovery. Pages 487-495.***

With the continuous exploitation of primary high-quality mineral resources, these resources could be gradually exhausted, so it is of great significance to recover iron-rich basic oxygen furnace (BOF) slag as secondary mineral resources. Given the composition characteristics of BOF slag, a method of synergetic modification of copper slag as additive and BOF slag was proposed to separate iron minerals for recovery. In this study, FactSage thermodynamic simulation, chemical analysis, X-ray diffraction and scanning electron microscopy were used to analyze the phase transformation and structure evolution during the oxidative modification process, and the effects of oxidation temperature and addition amount of copper slag on the modification were studied. The results show that the addition of copper slag can effectively promote the transformation of iron oxides to  $\text{MgFe}_2\text{O}_4$ . When an appropriate amount of copper slag was added to make the basicity of the mixed slag be 2, the conversion rate of  $\text{MgFe}_2\text{O}_4$ , iron recovery rate and grade of magnetic slag were the best. In the oxidative modification process, increasing the oxidation temperature was beneficial to the formation and development of  $\text{MgFe}_2\text{O}_4$ . However, too high temperature could lead to the dissolution of  $\text{Al}^{3+}$  into  $\text{MgFe}_2\text{O}_4$  and reduce its magnetism, which was not conducive to magnetic separation and recovery. When the mixed slag was modified at 1200 °C, the grade of magnetic slag by magnetic separation was 31.14 % and the recovery was 64.04 %, which had the

potential of returning to sintering or ironmaking. The secondary slag obtained at the same time can also be used to produce high value-added materials. Therefore, the current technological route can transform the two kinds of industrial solid waste into usable resources at the same time, and realize "waste treatment with waste".

- **Keywords:** Industrial BOF slag; Copper slag; Modification; Iron phase transformation; Magnetic separation

**Umair Baig, Shehzada Muhammad Sajid Jillani, Abdul Waheed, Mohammad Azam Ansari. *Exploring a combination of unconventional monomers for fabricating a hyper-cross-linked polyamide membrane with anti-fouling properties for production of clean water. Pages 496-504.***

A new hyper-cross-linked polyamide TFC NF membrane (M-I) was fabricated by using tetraethylenepentamine (TEPA) and terephthaloyl chloride (TPC). Fabricated membrane M-I was treated with 15 % hydrofluoric acid (HF) and membrane was regarded as M-2. Both membranes were thoroughly characterized by FESEM, ATR-FTIR, EDX analysis, Elemental mapping, and water contact angle (WCA). Performance of both membranes was evaluated in the form of permeate flux and rejection of Eriochrome Black T (EBT) along with salts (Na<sub>2</sub>SO<sub>4</sub>, MgSO<sub>4</sub>, MgCl<sub>2</sub>, NaCl and CaCl<sub>2</sub>) while anti-organic and antibiofouling performance of both of the membranes was studied by using Bovine Serum Albumin (BSA) as a model foulant while Escherichia coli and Staphylococcus aureus as model gram-negative and gram-positive bacterial strains. The membrane M-II showed better performance compared to the membrane M-I. The membrane M-II showed a permeate flux of 88.57 LMH at 24 bar with rejection of > 99 % of EBT and > 81 % of NaCl. The membrane M-II showed a decline in flux of merely 2.7 % with a flux recovery of 98.6 %. The bacteriostatic experiments demonstrated that the membrane M-II inhibited E. coli and S. aureus growth by 22.8 % and 77.5 %, respectively, after 24 h of incubation.

- **Keywords:** Bacteriostasis; Membrane; Polymer; Interfacial polymerization; Tetraethylene pentaamine; Terephthaloyl chloride

**Qingqing Wan, Jiaqi Bu, Zhiwei Deng, Hui Liu, Tianhao Li, Tong Luo, Chengyun Zhou, Shian Zhong. *Peroxymonosulfate activation by bimetallic modified syderolite pellets catalyst for degradation of brominobenzonitrile. Pages 505-513.***

In this study, syderolite (Sd) pellets loaded with bimetallic oxides (Sd-Ni-Co) catalyst was prepared for the first time, which was used to activate peroxymonosulfate (PMS) for the degradation of Brominobenzonitrile (BMN). The effects of the Sd-Ni-Co dose, PMS dose, pH value, BMN concentration, and different anions on the degradation experiment were explored. The optimal reaction conditions for the degradation of 50 mg/L BMN were 100 g/L Sd-Ni-Co and 0.2 g/L of PMS, and the degradation was complete at room temperature within 40 min. The ten continuous cycle test shows the perfect structural stability of Sd-Ni-Co. Sd-Ni-Co/PMS system not only shows a good degradation performance on BMN but also on other organics, indicating that the method has a good universality. The radical quenching experiments (ethanol and tert-butanol) show that both •OH and SO<sub>4</sub><sup>-</sup> play an important role in this reaction system, and further confirmed the result by electron paramagnetic resonance (EPR) spectra. The Sd-Ni-Co was characterized by SEM, XRD, XPS, and BET. The degradation process was analyzed by triple quadrupole liquid chromatography-mass spectrometry (LC-MS), and the possible degradation pathway and mechanism were proposed.

- **Keywords:** Syderolite; Bimetallic oxide; Advanced oxidation process; Peroxymonosulfate; Brominobenzonitrile

**Poongavanam Ganesh Kumar, V.S. Vigneswaran, K. Balaji, S. Vinothkumar, Rajendran Prabakaran, D. Sakthivadivel, M. Meikandan, Sung Chul Kim. *Augmented v-corrugated absorber plate using shot-blasting for solar air heater – Energy, Exergy, Economic, and Environmental (4E) analysis. Pages 514-531.***

Need for increasing the shelf life of agricultural produce using renewable energy based A decentralized system are significantly increasing. The solar air heating systems (SAHs) are efficient and environment friendly systems which are used for preserving agricultural produce through the reduction of moisture content. However, these systems had poor thermal efficiency and the way for increasing the efficiency are much need in the present era. This article presents the energy, exergy, and economic analysis of a modified solar air heater system (SAH). The proposed (modified) SAH has a V-corrugation absorber plate; the inner surface was modified using shot-blasting technology. This is the first study to experimentally investigate a modified SAH and compare the results with those of a conventional SAH. Additionally, an environmental and sustainability assessment of the SAH is presented. The SAH performance was tested at airflow rates ranging from 0.01 to 0.02 kg. sec<sup>-1</sup>. The proposed SAH achieved higher energy and exergy efficiencies (15% and 34%, respectively) than a conventional SAH at a flow rate of 0.02 kg. sec<sup>-1</sup>. Although the modification significantly improves the SAH performance, the performance must be further improved as the SAH has a low exergy efficiency. Through extensive experimental investigation, it was found that the modified SAH performs well in terms of energy, exergy, and economics. Pertaining to MFR of 0.01, 0.015, and 0.02 kg. sec<sup>-1</sup> the average energy efficiency of the modified SAH was increased by around 2.4%, 3.1%, and 5.8% greater than that of the conventional SAH, respectively. Concerning the MFR of 0.01, 0.015, and 0.02 kg. sec<sup>-1</sup> the average exergy efficiency (AEE) was augmented about 0.21, 0.36, and 0.70 higher in the modified SAH, respectively. With MFRs of 0.01, 0.015, and 0.02 kg. sec<sup>-1</sup>, the modified SAH system mitigates approximately 10.3 tons, 18.06 tons, and 28.7 tons of CO<sub>2</sub>/year, respectively. The enviroeconomic factors of the modified (shot blasted) SAH were augmented by about 23.4%, 15.1%, and 18.2% compared with the conventional SAH at MFRs of 0.01, 0.015, and 0.02 kg. sec<sup>-1</sup>, respectively.

- **Keywords:** Solar air heater; Shot-blasting; V-corrugation; Energy analysis; Exergy analysis; Economic analysis

**Fuyu Wang, Xuanyi Zhou, Jian Huang, Hengdong Wang, Hideki Kikumoto, Chengyun Deng. *Natural gas leakage estimation in underground utility tunnels using Bayesian inference based on flow fields with gas jet disturbance. Pages 532-544.***

In damp environment of underground utility tunnels, natural gas pipelines may corrode, resulting in leakage from small holes. Considering the flammable and explosive properties of natural gas, accurate and prompt identification of leakage location and leakage rate after gas leaks is crucial for emergency repair. Prior research assumed that source leakage causes no disturbance on its surrounding flow field. However, when natural gas leaks, the leaking gas may reach a very high speed in certain cases, which will produce a non-negligible disturbance on the surrounding flow field, causing a large error in source parameters estimation. In this paper, Bayesian inference for source parameters estimation is further developed based on the disturbed flow field. The results demonstrate that when the leakage rate is high, using undisturbed flow fields for estimation will lead to large errors (with the maximum error of about 46 %), whereas estimated results are closer to true values when using disturbed flow fields with the final

error within 5 %. Finally, the dimensionless leakage rate is used as a metric to quantify the disturbance effect. It is considered that disturbed flow fields are needed for source parameters estimation when the dimensionless leakage rate is above 1.

- **Keywords:** Source parameters estimation; Bayesian inference; Disturbed flow field; Natural gas leakage; Adjoint equations

**Abdullah Anwar, Xuemei Liu, Lihai Zhang. *Biogenic corrosion of cementitious composite in wastewater sewerage system - A review.* Pages 545-585.**

Biogenic corrosion of concrete in wastewater systems is a severe and widespread global problem, costing billions of dollars in annual maintenance and rehabilitation. Corrosion of cementitious matrix due to the in-situ formation of sulfuric acid ( $H_2SO_4$ ) by the colonization of sulfur-oxidizing bacterial species on concrete surfaces is considered the primary cause of structural degradation. In its advanced stage, corrosion may even lead to structural failure within 10–20 years and jeopardize its durability. Despite the significant efforts made by researchers worldwide toward different repair approaches, the problem of biogenic corrosion of cementitious composites remains unresolved and a challenge for industries and stakeholders. Currently, cement composites are not able to carry out prolonged acidic attacks in sewerage systems ( $pH < 3$ ), which stimulates the urgent need for improved research. The purpose of this research article is to provide an in-depth analysis of how the biogenic sulfuric acid (BSA) attack initiated and propagated concrete deterioration at various levels of the processes involved. Additionally, the article presented some of the previous case studies and preservation measures adopted to reduce concrete corrosion in wastewater sewerage systems.

- **Keywords:** Biogenic sulfuric acid attack; Concrete; Corrosion; Durability; Hydrogen sulfide; Wastewater system

**Yuan Han, Houcheng Zhang, Fu Wang, Jiapei Zhao, Chunfei Zhang, He Miao, Jinliang Yuan. *Synergistic integration of molten hydroxide direct carbon fuel cell and Stirling heat engine for efficient and clean coal use.* Pages 586-596.**

To reuse the exhaust heat produced by molten hydroxide direct carbon fuel cells (MHDCFCs), a new combined system mainly composed of an MHDCFC, a regenerator, and a Stirling heat engine (SHE) is theoretically integrated for fuel-to-power efficiency enhancement. Mathematical formulas of the performance indicators for the combined system are derived based on the first and second laws of thermodynamics, from which the feasibility and effectiveness of the combined system are evaluated from both energetic and exergetic viewpoints. Moreover, the optimum working regions of the combined system are further specified by using a multi-objective function paying equal attention to both efficiency and power output. Results show that SHEs can be effectively acted as bottoming cycles for MHDCFC for additional mechanical power production. Numerical calculations indicate that the maximum power density and its corresponding energy efficiency and exergy efficiency of the proposed system are, respectively, about 97.6%, 97.1% and 99.2% greater than that of the single MHDCFC. Furthermore, extensive parametric studies show that increasing working temperature, volume ratio, hot-side working substance temperature or mean pressure is beneficial for the overall system performance, while increasing reactor compartment width may degrade the overall system performance.

- **Keywords:** Molten hydroxide direct carbon fuel cell; Stirling heat engine; Combined system; Energetic; Exergetic



**Borna Bayat, Kambiz Tahvildari, Alireza Hemmati, Amin Bazayari, Ahad Ghaemi. *Production of ethylene glycol monobutyl ether through etherification of ethylene glycol using a nanostructured heterogeneous catalyst of amyberlyst-15. Pages 597-609.***

This work aims to produce butyl glycol from the etherification of ethylene glycol (EG) and n-butanol (NB) using different heterogeneous Amyberlyst-15 catalysts in a pressurized reactor tank. Experiments were designed by response surface methodology according to the central composite design (RSM-CCD). Three operating conditions of temperature (140–200 °C), reaction time (2–22 h), and EG: NB molar ratio (1:1–1:9) were considered to model and optimize the EG conversion under fixed pressure and catalyst weight. A quadratic conversion model was proposed as a function of independent and combined studied parameters, predicting the experimental data with high accuracy ( $R^2 > 0.98$ ). According to the response surface results, all variables positively affected the response. The optimal reaction condition for maximizing conversion was at 1:8.2, 4.1 h, and 200 °C, achieving the EG conversion of 86.12 %. Furthermore, the catalyst reusability was checked after four cycles, indicating a reduction of about 15 % in conversion after each cycle. The FESEM, FTIR, XRD, BET, and TGA analyses characterized the fresh catalyst and used catalyst after the fourth cycle. Both samples had a spherical morphology, and the used catalyst contained carbon-based sediments, intensifying the stretching vibration of C-O bond peaks. The pore diameter and volume of the fresh catalyst were 18.93 nm and 2.38 cm<sup>3</sup>/g, respectively, while these values were 22.07 nm and 0.36 cm<sup>3</sup>/g for the used catalysts after the fourth cycle. The reduction in the catalytic activity of the used sample can be because of the pore deformation.

- **Keywords:** Ether glycol monobutyl ether; Etherification; Amyberlyst-15 catalyst; Ethylene glycol; Response surface methodology

**Xinyue Song, Fengyan Li, Tao Yan, Feng Tian, Linlin Ren, Chengfang Jiang, Qi Wang, Shusheng Zhang. *Research progress in the sample pretreatment techniques and advanced quick detection methods of pesticide residues. Pages 610-622.***

The wide use of pesticides has caused serious environmental pollution and posed many potential health hazards. Therefore, it is of great importance to develop feasible, fast and accurate analysis methods for pesticide residues detection. Generally, pesticide residues exist in complex sample matrices and their concentrations are around µg/mL-ng/mL. Thus, sample pretreatment techniques are indispensable which could eliminate the interfering substances in the sample matrix, enrich analytes to reach to the detection level of analytical equipments, obtain the detection results with higher reliability and accuracy. Thus, this review mainly discussed the widely-used sample pretreatment techniques and advanced quick analysis methods for pesticides residues detection, then the prospects for pesticide residues analysis was proposed.

- **Keywords:** Enrichment; Microextraction; Pesticide residues; Rapid detection; Sample pretreatment

**Kevin Chau, Abdoulaye Djire, Sreeram Vaddiraju, Faisal Khan. *Process Risk Index (PRI) – A methodology to analyze the design and operational hazards in the processing facility. Pages 623-632.***

Process safety assists in improving the operational, economic, and environmental performance of processing facilities. This study addresses the critical process safety challenges at the process design and operation stage through an effective risk minimization strategy. The process risk index (PRI), a heuristic-based approach, is used to map risk and explore the effect of process deviations on process safety. The PRI

method is explained using the blue hydrogen process - steam methane reforming (SMR) process. A risk map of the entire facility uses traffic-light colors as risk indicators is developed. The synergistic effects and parameters are analyzed using process simulation tools and converted into risk values. The risk map identifies the reforming, the water-gas shift, and the separator units as the highest risk units for given deviations in the operational parameters. We have benchmarked the PRI with the fire and explosion damage index (FEDI) and observed that the PRI is more sensitive to finding process deviations and hazards. This method can detect root causes of process safety issues at a unit-specific level better than the FEDI. Additionally, the PRI provides updated risk maps once risk minimization strategies are implemented. The PRI serves as a tool for process safety analysis of hazardous operations such as hydrogen production processes with better sensitivity and flexibility in scaling.

- **Keywords:** Process Safety; Hydrogen Safety; Operational Hazards; Risk Assessment; SMR Process

**Yawei Lu, Xingyan Cao, Zhirong Wang, Shuoxun Shen. *Oxidative self-heating modeling of iron sulfides during the processing of high sulfur oil.* Pages 633-645.**

Scanning electron microscope (SEM), energy dispersive spectroscopy (EDS) and X-ray diffraction (XRD) were used to analyze the surface micromorphology and components of the iron oxide sulfide powders respectively. Differential scanning calorimetry (DSC) and thermogravimetry (TG) were used to investigate the self-heating properties. It was observed that temperature had a significant effect on the microscopic morphology and composition of the sulfide products. The product powders were homogeneously distributed in small particles and the composition of the products were converted from non-stationary FeS to FeS<sub>2</sub> with the sulfidation temperature increased. The apparent activation energy at a sulfidation temperature of 300 °C was 66.5 % of that at a sulfidation temperature of 150 °C. The apparent activation energies were 114.65 kJ/mol, 95.41 kJ/mol, 89.5 kJ/mol and 76.27 kJ/mol respectively at 150 °C, 200 °C, 250 °C and 300 °C during the self-heating reaction phase. There was only one main weight loss phase for the 100 °C, 150 °C and 200 °C products, while the 250 °C and 300 °C products had an additional weight loss phase before the main weight loss phase. The apparent activation energies of the main weight loss phase of the five temperature products were 318.1–333.7 kJ/mol, 266.2–293.2 kJ/mol, 212.7–234.0 kJ/mol, 174.7–193.1 kJ/mol and 168.7–188.7 kJ/mol, respectively. The apparent activation energies of the first weight loss phase of the 250 °C and 300 °C products were 217.4–243.2 kJ/mol and 198.2–214.6 kJ/mol respectively. The mechanism function for the thermal oxidation of elemental sulfur in the first weight loss phase was determined to follow the spherical contraction phase boundary reaction model, i.e.  $g(\alpha) = [1-(1-\alpha)^{1/3}]^m$ . In the main weight loss phase, the mechanism function for the thermal oxidation of iron sulfate followed the random nucleation followed by subsequent growth model, i.e.  $g(\alpha) = [\ln(1-\alpha)]^m$ .

- **Keywords:** Sulfide products; Temperature rise rate; Oxidative self-heating; Pre-exponential factor; Kinetic model

**Chao Zhang, Youzhi Liu, Weizhou Jiao, Guisheng Qi, Jing Guo. *A turbulent mass diffusivity model for the simulation of the biodegradation of toluene in an internal loop airlift reactor.* Pages 646-657.**

In this study, a three-dimensional computational fluid dynamics model is established in Ansys Fluent to describe the biodegradation of toluene in an internal loop airlift reactor (IALR). The Euler-Euler approach is used with the standard k- $\epsilon$  method to predict the

hydrodynamics of the reactor, and the population balance model is used to describe the bubble size distribution in the reactor. The recently developed concentration variance  $c_2^2$  and its dissipation rate  $\epsilon c$  formulations are adopted to close the turbulent mass transfer differential equations, so that the turbulent mass diffusivity can be determined without using empirical methods. There is a good agreement between the simulated dissolved oxygen concentrations obtained by the proposed model and the experimental data reported in the literature. As the predicted turbulent mass diffusivity is found to be unevenly distributed and the calculated turbulent Schmidt number  $S_{ct}$  is not a constant but varies, it may not be appropriate to use a constant  $S_{ct}$  or an experimentally determined dispersion coefficient. In addition, the maximal shear stress is found in the top region of the IALR and the liquid flow are very uniform in the riser and downcomer.

- **Keywords:** Internal loop airlift reactor; Computational fluid dynamics; Shear stress distribution; Turbulent mass diffusivity; Biodegradation

**Yue Wu, Xing Yu, Zongcheng Wang, Hao Jin, Yanqiu Zhao, Changjian Wang, Zhihe Shen, Yi Liu, Wei Wang. *The flame mitigation effect of N<sub>2</sub> and CO<sub>2</sub> on the hydrogen jet fire. Pages 658-670.***

Hydrogen has attracted much attention from governments and enterprises around the world due to its zero pollution and recycling use. However, it may bring safety problems such as hydrogen jet fire due to its wide flammability range and low ignition energy. Therefore, the methods of preventing hydrogen jet fire need to be explored urgently. In order to investigate the effect of gaseous fire extinguishing agent on the hydrogen jet fire, a series of experiments were carried out to study the flame behaviors under the effects of nitrogen and carbon dioxide jets. The fire extinguishing agents were released through a jet nozzle with diameter of 3 mm at the pressure of 11 atm. The flame length, thermal radiant flux and total heat flux were analyzed. The results show that the reduction ratio of vertical flame length increases with the decrease of the installation height of the extinguishing agent nozzle. It indicates that when the fire extinguishing agent is injected at the root of hydrogen jet flame, the fire may be extinguished. Due to the reduction of flame size, the thermal radiant flux received by the radiometer decreases, which corresponds to the reduction of flame radiation fraction. The total heat flux received in the downstream region of deflected flame is determined by the joint action of thermal radiation and convection. The convective heat transfer of high-temperature gas may cause the value measured by the heat flux meter on the flow path of the deflected flame to increase. Besides, the extinguishing limit for hydrogen jet flame under the effects of nitrogen and carbon dioxide jets are analyzed.

- **Keywords:** Hydrogen safety; Hydrogen jet flame; Fire extinguishing agent; Nitrogen; Carbon dioxide

**Alain Ginestet, Mirela Robitu, Lionel Boiteux. *Design improvement of an injection pipe and its validation on the performances of a semi-industrial pulse-jet baghouse. Pages 671-679.***

The purpose of this study is to improve the operation of a pulse-jet baghouse by the modification of the design of its compressed air injection pipe. The base injection pipe has all the nozzles of constant diameter (9.7 mm). To characterise the injection pipe, experimental measurements and three dimensional CFD simulations were carried out. The impact of the geometry of the injection pipe on the behaviour of an instrumented filter bag moved under the nozzles has been assessed from experimental measurements. Once the design of a new injection pipe has been defined by three dimensional CFD simulation and assessed by measurements, the performances of a semi-industrial pulse-jet baghouse has been measured with both the base and the modified injection pipes. The main conclusion of our study is that in order to ensure that cleaning of filter bags belonging to the same injection pipe is more homogeneous, it is not enough to assess

the injection pipe (by measurements and/or calculation) but it is also necessary to characterize the behaviour of a filter bag moved under and along the nozzles of the injection pipe. The results of our study show that a new injection pipe geometry with decreasing nozzle diameter (from 10.5 mm at the inlet to 8.0 mm at the bottom of the pipe) allows a more uniform behaviour of the instrumented filter bag moved under and along the pipe. This better uniformity is characterized by both the average peak pressure and the average root mean square acceleration averaged along the height of the filter bag. Finally, when operated with the modified injection pipes, the semi-industrial pulse-jet baghouse shows better performances characterized by lower residual pressure drop after cleaning (-8 %), longer filtration cycles (+70 %) and lower particle emissions (-5 % for PM<sub>1</sub>, -15 % for PM<sub>2.5</sub> and -18 % for PM<sub>10</sub>).

- **Keywords:** Dust collector; Nozzle diameter; Cleaning uniformity; Baghouse; Filtration; Computational fluid dynamic

**Jialong Zhu, Zhong Wang, Ruina Li. *Experimental study on particle microstructure of diesel/biodiesel blend fuels measured by SAXS and HRTEM techniques. Pages 680-693.***

In order to investigate the mechanism on the microstructure of soot by adding biodiesel to diesel, the soot of biodiesel/diesel mixed fuel was collected by a constant volume combustion chamber, and the microstructure characteristics of soot were studied by SAXS and HRTEM techniques. The results showed that the added biodiesel reduced the delay of ignition and advanced the peak time of soot generation. The particulate matter in soot underwent a deep internal and external oxidation process. The accumulation of internal oxidation products forms a certain filling effect, which affects the subsequent oxidation rate. The microstructure of the single particulate matter was further refined to a cylindrical-like 3D sub-model filled with voids. The improved sub-model optimizes the DPF pressure drop model and provides a potential research basis for the DPF catalytic oxidation and regeneration model.

- **Keywords:** Biodiesel; Soot; Microstructure; SAXS; HRTEM

**Kwanghwi Kim, Hyunji Lim, Hyun Sic Park, Jo Hong Kang, Jinwon Park, Hojun Song. *Effect of amino acid additives in ammonia solution on SO<sub>2</sub> absorption and ammonia escape using bubbling reactor for membrane contactor applications. Pages 694-703.***

Controlling the SO<sub>2</sub> emissions is crucial because they result in several environmental problems and affect human health. Several techniques have been proposed for controlling SO<sub>2</sub> emissions. Limestone or lime-based absorbents are widely used for SO<sub>2</sub> removal. However, their low solubility limits their applications. Ammonia solution has attracted attention owing to its higher SO<sub>2</sub> removal efficiency. However, owing to its high volatility, it has the propensity to escape, which can cause secondary environmental pollution. Therefore, we investigated the effect of six amino acid additives to improve the SO<sub>2</sub> absorption performance and inhibit the ammonia escape in aqueous ammonia solution. The surface tension and theoretical breakthrough pressure of the amino acid-containing ammonia solutions was investigated to evaluate their applicability to a membrane contactor process. L-histidine (His) exhibited the best performance. Therefore, the effect of His concentration, inlet SO<sub>2</sub> concentration, and absorption temperature on SO<sub>2</sub> absorption performance was explored. The <sup>13</sup>C nuclear magnetic resonance (NMR) and <sup>1</sup>H NMR analyses were used to study the SO<sub>2</sub> absorption mechanism. This study provides a strategy for preparing an eco-friendly and highly efficient SO<sub>2</sub> absorbent that can overcome the disadvantage of current ammonia solutions for the removal of low-concentration SO<sub>2</sub> from industrial gas emissions for the membrane contactor process application.

- **Keywords:** Sulfur dioxide absorption; Flue gas desulfurization; Amino acid additives; Ammonia escape; Membrane contactor

**Yongjie Fan, Jing Yang, Kaicong Cai, Zhilei Lu, Jiejie Chen, Xingteng Lai, Zeping Xu, Zhenle He, Yuyi Zheng, Changqing Liu, Qiyuan Sun, Rongkun Jian, Feifeng Wang. *Mechanism of 9,10-Dihydro-9-oxa-10-phosphaphenanthrene-10-oxide degradation in UV light-emitting diodes lamp driven sodium sulfite activation process.* Pages 704-715.**

DOPO (9,10-Dihydro-9-oxa-10-phosphaphenanthrene-10-oxide) is emerging organic phosphorus flame retardant, which has gained greatly attention because of its adverse health effects on aquatic organisms. In this study, UV light-emitting diodes lamp driven sodium sulfite activation (UV254/Sulfite) process was employed as an advanced reduction process to remove DOPO, and its mechanisms were revealed. The pseudo first order rate constant of DOPO ( $k_{obs-DOPO}$ ) in UV254/Sulfite process initially decreased from  $6.95 \times 10^{-5} \text{ s}^{-1}$  to  $5.11 \times 10^{-5} \text{ s}^{-1}$ , and subsequently increased to  $1.61 \times 10^{-4} \text{ s}^{-1}$  as the sulfite concentration increased from 0 to 10 mM, indicating that the negative effect of  $\text{HSO}_3^-$  on DOPO degradation was the dominate factor in UV254/Sulfite process at low sulfite concentration ( $< 2 \text{ mM}$ ), while the yields of hydrated electron ( $\text{eaq}^-$ ) increased as the sulfite concentration gradually reaching to a high value (10 mM), resulting in enhancing DOPO degradation significantly. In addition, the coexisted water matrix in deionized water and natural surface water weakened DOPO degradation in UV254/Sulfite process, and this inhibition strengthened as the concentrations of water matrix raised. The DOPO degradation pathway indicated that  $\text{eaq}^-$  attacked phosphaphenanthrene structure of DOPO and contributed to its detoxification which was confirmed by Quantitative Structure-Activity Relationship (QSAR) assessment.

- **Keywords:** DOPO degradation; Hydrated electron; UV254/Sulfite; Advanced reduction process (ARP); Products toxicity

**Júlia do Nascimento Pereira Nogueira, Príamo Albuquerque Melo, Maurício B. de Souza Jr. *Faulty scenarios in sour water treatment units: Simulation and AI-based diagnosis.* Pages 716-727.**

Fault Detection and Diagnosis (FDD) is a Process System Engineering (PSE) area of great importance, especially with increased process automation. It is one of the chemical engineering fields considered promising to Artificial Intelligence (AI) application. FDD systems can be useful to supervise Sour Water Treatment Units (SWTU) behavior, as they are chemical processes that present operational difficulties when disturbances occur. SWTU remove contaminants from sour water (SW) streams generated through petroleum processing, consisting mainly of small amounts of  $\text{H}_2\text{S}$  and  $\text{NH}_3$ . They are considered one of the primary aqueous wastes of refineries and cannot be disposed of due to environmental regulations. However, no previous studies focused on the development of FDD systems for SWTU exist and works on its dynamics are scarce. Hence, the present work proposes to study the dynamic simulated behavior of an SWTU and develop an FDD system applying AI techniques with hyperparameters optimization. The simulation was performed in Aspen Plus Dynamics® and ran to create normal operation and six relevant faults, including occurrences in the process (e.g., inundation and fouling) and sensors. FDD was performed through data classification, and results were evaluated mainly by accuracy and confusion matrices. Even after variable reduction, FDD was satisfactory with over 87.50% accuracy in all AI techniques. RF and SVM with linear and Gaussian kernels presented the best results, with over 93% of accuracy in training and testing, and had the shortest computing times. The second column's sump level proved to be the most relevant variable for fault identification.

- **Keywords:** Dynamic simulation; Sour water treatment units; Faulty scenarios; Machine learning; Random forests; Support vector machines; Deep neural networks

**Zhihong Gao, Junfeng Su, Amjad Ali, Yihan Bai, Yue Wang, Qiao Chang. Accelerated reduction of nitrate by driving the manganese (Mn) cycle process with dissimilatory Mn reducing bacteria: Differential reduction pathways and cycling mechanisms. Pages 728-738.**

The coupling of microbial dissimilatory manganese (Mn) reduction and nitrogen transformation in anaerobic environment affects the fate of many elemental geochemical cycles. A strain of dissimilatory manganese reducing bacteria (DMRB) named *Pantoea* sp. MFG10 was isolated for simultaneous reduction of Mn(IV) oxides and NO<sub>3</sub><sup>-</sup>-N to explore the differential reduction mechanism. The post-reaction precipitates were investigated for researching potential persistent products. The strain MFG10 could achieve 99.86% NO<sub>3</sub><sup>-</sup>-N removal (1.176 mg L<sup>-1</sup> h<sup>-1</sup>) and 20.97 mg L<sup>-1</sup> (0.583 mg L<sup>-1</sup> h<sup>-1</sup>) free Mn(II) yield within 12 and 36 h, respectively. The transient intermediate Mn(III) formed after the reduction of strain MFG10 was utilized in the denitrification process. The restricted Mn reduction behavior in the NO<sub>3</sub><sup>-</sup>-N and manganese oxide co-reduction system led to the formation of large amounts of Mn(III) by single electron transfer of Mn(IV). Mn(III) acts as electron donor and re-oxidized to constitute a dynamic manganese cycle pathway. Thus, the addition of manganese oxide significantly improved the denitrification efficiency and the fast electron flow formed an abundant Mn(III) secondary minerals on the surface of the manganese oxide. This work will help to understand the more subtle environmental and process-based manganese cycle and inspire new strategies to develop efficient manganese recycling processes for groundwater pollution control.

- **Keywords:** Dissimilatory manganese reducing bacteria; Groundwater contamination; Manganese cycle; Manganese oxides; NO<sub>3</sub><sup>-</sup>-N removal

**Salah Meddah, Mohamed El Hadi Samar, Mohamed Bououdina, Lotfi Khezami. Outstanding performance of electro-Fenton/ultra-violet/ultra-sound assisted-persulfate process for the complete degradation of hazardous pollutants in contaminated water. Pages 739-753.**

This work focuses on the degradation of the hazardous azo dye Naphthol Blue Black (NBB) utilizing an innovative approach combining electro-Fenton (EF), ultra-violet (UV), and ultra-sound (US) processes while varying the operating parameters (concentration of iron and dye, pH, current intensity). Under the optimum experimental conditions, an excellent degradation efficiency of the NBB dye is achieved after 60 min, i.e., 98%, 95%, and 65% for EF, UV, and US processes, respectively. The addition of persulfate significantly improves the efficiency and accelerates the kinetics of the NBB degradation. Combining all processes assisted with persulfate achieved 99% NBB degradation within a very short contact time of 2 min and 98% reduction in COD after 55 min. The as-obtained outstanding performance associated with the synergistic effects of EF/US/UV alongside the addition of persulfate can be adopted to degrade other hazardous substances.

- **Keywords:** Water treatment; Advanced oxidation; Degradation; Naphthol Blue Black; Persulfate ions; Hydrogen peroxide

**G.V. Kuznetsov, A.O. Zhdanova, R.S. Volkov, P.A. Strizhak. *Optimizing firefighting agent consumption and fire suppression time in buildings by forming a fire feedback loop.* Pages 754-775.**

The paper presents experimental research findings for the characteristics of physical and chemical processes in the seat of fire at different stages of fire development and suppression. Combustion product temperatures and composition, as well as the luminous intensity of the flame were recorded. The research was carried out using a model of class A fire. The most effective combinations of technical equipment were determined that are necessary and sufficient for early fire detection, timely suppression initiation, combustion and smoldering completion. The minimum volumes of a firefighting liquid (water) necessary and sufficient to suppress combustion were determined. The benefits of using feedback systems during firefighting were substantiated. These systems optimize the consumption of fire-extinguishing agents and time of fire suppression by monitoring the fire behavior in real time. Recommendations were made on the engineering of automatic indoor fire suppression systems that optimize the conditions of firefighting and minimize threat to people's lives and health.

- **Keywords:** Compartment fires; Fire suppression; Continuous control of fire behavior; Early fire detection; Feedback systems; Automatic fire monitoring and suppression systems

**Rouzbeh Abbassi, Ehsan Arzaghi, Mohammad Yazdi, Vahid Aryai, Vikram Garaniya, Payam Rahnamayiezekavat. *Risk-based and predictive maintenance planning of engineering infrastructure: Existing quantitative techniques and future directions.* Pages 776-790.**

Engineering infrastructure incorporate complex systems, hazardous materials and often operated by human beings, making them prone to catastrophic accidents. Continuously improving system safety of the facilities and their operations requires a well-established asset management practices. The history of hazardous events in some domains such as process facilities suggest that many accidents have occurred due to ineffective maintenance planning strategies. Thus, to ensure an acceptable level of system safety and availability, it is essential to adopt optimal programs and practical procedures in maintenance planning engineering assets. The lessons learnt from previous accidents have helped operators, classification societies and regulators to develop viable standards and guidelines for employing quantitative methods in Operation and Maintenance (O&M) planning. The current work aims to present the existing attempts and identify the gaps, needs, and challenges of maintenance planning in engineering facilities. It then integrates the empirical and theoretical conclusions, highlighting the capabilities and drawbacks of the state-of-the-arts and explaining research opportunities and challenges. The decision-makers, operators, and managers in engineering infrastructure can exploit the present work from theoretical and practical perspectives.

- **Keywords:** Maintenance operations; Process industry; Risk analysis; System safety; Decision-making

**Alain Islas, Andrés Rodríguez Fernández, Covadonga Betegón, Emilio Martínez-Pañeda, Adrián Pandal. *Computational assessment of biomass dust explosions in the 20L sphere.* Pages 791-814.**

Determination of the explosion severity parameters of biomass is crucial for the safety management and dust explosion risk assessment of biomass-processing industries. These are commonly determined following experimental tests in the 20L sphere according to the international standards. Recently, CFD simulations have emerged as a reliable alternative to predict the explosion behavior with good accuracy and reduced labor and

capital. In this work, numerical simulations of biomass dust explosions are conducted with the open-source CFD code OpenFOAM. The multi-phase (gas-solid) flow is treated in an Eulerian-Lagrangian framework, using a two-way coupling regime and considering the reactions of biomass conversion (moisture evaporation, devolatilization, and char oxidation), the combustion of volatile gases, and convective and radiative heat transfer. The model is validated with pressure-time and concentration-dependent experimental measurements of two biomass samples. Results suggest that the characteristics of the cold-flow (i.e., turbulence levels, actual dust concentration, spatial distribution of the dust cloud, and turbophoresis effect) govern the course of the explosion process, and depend strongly on particle size, dust concentration, and ignition delay time effects. These findings may be relevant in the design of better dust explosion testing devices and to the reexamination of the guidelines for the operation of the experiment. Finally, a thorough discussion on the explosion pressures, degree of biomass conversion, flame temperature, flame propagation patterns, and the dust agglomeration effect is presented.

- **Keywords:** Dust explosions; Biomass; CFD; OpenFOAM

**Z. Fallahnejad, Gh. Bakeri, A.F. Ismail. *Overcoming the trade off between the permeation and rejection of TFN nanofiltration membranes through embedding magnetic inner surface functionalized nanotubes*. Pages 815-840.**

Today, one of the most important environmental problems is the treatment of industrial wastewaters containing heavy metal ions and salts. In this research, thin-film nanocomposite (TFN) membranes were developed through incorporation of modified titanate nanotube (TNT) and halloysite nanotube (HNT) into the polyamide (PA) active layer to improve the performance of the NF membranes. At first, the internal surface of the nanotubes was coated with different polymers to lessen the inner diameter of the nanotubes. Then, the inner surface coated nanotubes were magnetized through placing Fe<sub>3</sub>O<sub>4</sub> on their outer surface. In case of magnetized nanotubes, the fabrication of the membranes was done in the absence and in the presence of the external magnetic field, which made the nanotubes to align in a regular pattern across the PA layer, smoothing the membranes' surface and lowering the contact angle. It is expected that the magnetized nanotubes can make suitable arrangement in the structure of thin layer in the presence of the magnetic field and show better performance. The nanotubes act as the channels for water transport and in case of inner coated nanotubes, reject more ions through the steric hindrance. The pure water permeation of the membranes, modified with polystyrene inner coated TNT and HNT increased by 71.23% and 80.27%, respectively compared to the pristine TFC membrane without any significant changes in the rejection of Na<sup>+</sup> and Cu<sup>2+</sup>; a suitable trade-off between the permeation and the ion rejection. In addition, the membranes modified by magnetized polyaniline inner coated TNT and HNT showed 36.24% and 75.62% more water permeation compared to the pristine TFC membranes while the rejections of Na<sup>+</sup> and Cu<sup>2+</sup> have not been changed remarkably. The results of this research showed that inner coating and magnetization of the nanotubes can be considered as a novel method to enhance the efficiency of TFN membranes for wastewaters treatment.

- **Keywords:** Inner surface coating; Magnetized nanotubes; Thin film nanocomposite membrane; Nanofiltration; Heavy metal ions separation

**N.B. Karthik, K.C. Bal Krishna, Stuart J. Khan, Arumugam Sathasivan. *A new chloramine recovery method in nitrifying water without "chlorine burn"*. Pages 841-850.**

A better alternative to breakpoint chlorination (BPC) or "chlorine burn" to recover from nitrification is proposed. The BPC involves adding chlorine to achieve Cl/N mass ratios



more than 7.5 g-Cl<sub>2</sub>/g-NH<sub>4</sub><sup>+</sup>-N to convert to free chlorinated system. Thus, it is operationally complex and increases the chance of the formation of regulated disinfection by-products (DBPs). Reverting the system back to (mono)chloraminated system is also operationally complex. All these processes require informing public and disruption to service. We tested three Cl/N mass ratios (5.5:1, 7.5:1, 10:1) and three predetermined reaction times (breakpoint reaction time). After the breakpoint reaction time, the samples were rechloraminated (2.5 mg/L at a Cl/N mass ratio of 4.5:1) twice. The second rechloramination was carried out when chloramine had reached 1.0 mg/L. The improvement was evaluated based on the ability of the method to improve chloramine stability, suppress nitrification, and reduce active bacterial cells. Results showed a Cl/N ratio of 5.5:1 (a new method) followed by two rechloramination doses achieved the same improvement as the traditional Cl/N ratio of 10:1 and one rechloramination. Major factor controlling the effectiveness of the new method relies on the ability of the disinfectant to deactivate chloramine-decaying proteins present in nitrified water. The new method does not need the conversion to a free chlorinated system and thus significantly minimises the operational complexity, disruption to service and potential to form DBPs. It offers a potentially novel solution but needs optimisation and testing in a continuous flow system.

- **Keywords:** Chloramine; Nitrification; Breakpoint chlorination; Water supply system; Bacterial regrowth

**Ningning Ding, Yufei Ji, Qiyue Kuang, Xin Wang, Zejun Zhou, Zhaoji Zhang. *Changes in shale gas produced water DOM during its early storage period: Molecular composition correlated with microbial functions.* Pages 851-859.**

The environmental problem posed by shale gas wastewater has received considerable research attention. Researchers mostly focus on the technical aspect of terminal centralized treatment with little concern on the topic of early collection and on-site pretreatment of PW near gas gathering stations. In this study, the short-term fluctuations of the DOM molecular composition and the concurrent transformation of the microbial community and functions were carefully examined when the PW was temporarily stored in a simulated reservoir near gas wells. Ultra-high resolution mass spectrometry was used to determine the molecular structure of the DOM samples. The data showed that during the short-term storage of PW, strongly polarized and nonvolatile organic compounds developed a complex molecular structure, resulting in molecules that were more unsaturated and lower bioavailability. Microbial activity was responsible for the changes in organic matter composition that occurred in the later stages of the storage process, during which the amount of nitrogenous organic molecules increased. Network analysis offered vital information on microbial functions related to organic matter composition and the patterns of interaction between them. Organic molecule consumption and accumulation were intimately connected to the interactions between various bacteria the same as the consumption and accumulation of DOM molecules.

- **Keywords:** Shale gas produced water; Early collection; Dissolved organic matter; High-resolution mass spectrometry; Network analysis

**Tianyu Ge, Qinghua Dong, Yan Liu, Boyang Li, Wenshuai Bai. *Comparison of runaway criteria for prediction of different thermal behaviors in the acetic anhydride hydrolysis reaction performing in batch or semi-batch reactors.* Pages 860-871.**

In this paper various runaway criteria for batch reactors (BRs) and semi-batch reactors (SBRs) have been used and compared to study the boundaries of different thermal behaviors for the acetic anhydride hydrolysis reaction with the solvent of acetic acid carried out in BRs and SBRs. It is shown that the majority of criteria for BRs could give

relatively precise results, but the remaining minority are less accurate due to they all have some specific assumptions. Besides, the simulated results indicated that all the criteria for SBRs could accurately identify the transition point from TR to QFS behaviors in spite of that they give slight different results of transition point corresponding to NI and TR behaviors. The results can give an effective instruction for selection and usage of runaway criteria, especially in terms of effectiveness and applicability, to easily identify thermal behaviors in chemical industry.

- **Keywords:** Runaway criteria; Acetic anhydride hydrolysis reaction; Thermal behaviors; Thermal runaway; QFS

**Déborah L. Villaseñor-Basulto, Abudukeremu Kadier, Raghuveer Singh, Ricardo Navarro-Mendoza, Erick Bandala, Juan M. Peralta-Hernández. *Post-tanning wastewater treatment using electrocoagulation: Optimization, kinetics, and settlement analysis. Pages 872-886.***

Post-tanning process in the tannery industry generates complex wastewater. Continuous electrocoagulation (EC) with carbon-steel electrodes was used to treat synthetic/post-tanning wastewater. Research surface methodology, based on central composite design (RSM-CCD), was used for variables optimization and analysis of variance (ANOVA) to relate all parameters. Optimal variables were identified as initial pH 3.0, current density 6.4 mA m<sup>-2</sup>, initial dye concentration 125 mg L<sup>-1</sup>, NaCl concentration 1000 mg L<sup>-1</sup>, and inlet flow rate 176 mL min<sup>-1</sup> to produce 71% dye removal, operational costs (OC) 0.05 US\$ m<sup>-3</sup>, power consumption 1.3 kWh m<sup>-3</sup>, iron consumption 0.05 kg m<sup>-3</sup>, dye removal capacity per dissolved mg iron (qe) 4.3 mg Dye L<sup>-1</sup> C<sup>-1</sup> and total dissolved solids (TDS) removal 43.5%. Best process conditions were used to treat real post-tanning wastewater and resulted in carbon oxygen demand (COD) and TDS abatement (23% and 76%, respectively), as well as low OC (0.84 US\$ m<sup>-3</sup>) and energy consumption (20.6 kWh m<sup>-3</sup>). Pseudo-first-order kinetic model was found fitting experimental results, having electrical energy per order (EEO) of 1 kW h m<sup>-1</sup> order<sup>-1</sup> with a higher k = 1.14 min<sup>-1</sup>. Scanning electron microscopy analysis suggested the presence of iron nanoparticles within the sludge. All input and output parameters resulted in statistically significant where TDS and qe were the most valued for effective pollutant removal optimization and prevention of TDS increase in treated water. The outcomes of this study suggest EC as a suitable treatment for post-tanning wastewater and further knowledge of steel-carbon EC reactor design and sludge reusing purposes.

- **Keywords:** Post-tanning process; Steel-carbon electrodes; Sludge reuse; Electrocoagulation; RSM

**Na Liu, Yiwen Mou, Kunyang Su, Xue Li, Tianxiang Lu, Wenbao Yan, Mingming Song, Ze Yu. *The effect of salinity stress on the growth and lipid accumulation of Scenedesmus quadricauda FACHB-1297 under xylose mixotrophic cultivation. Pages 887-894.***

In the commercial production of microalgae biodiesel, high culture cost and low lipid production yields are two major limitations. Finding cheap carbon sources and ways to promote lipid accumulation can achieve low-cost cultivation and efficient lipid production. The impact of NaCl on the growth and lipid accumulation in *Scenedesmus quadricauda* FACHB-1297 under xylose mixotrophic cultivation was explored in this study. The results showed that when NaCl concentration were 0.88–5.85 g/L, the biomass concentration and lipid content were 2.15–2.68 and 1.19–1.80 times higher than those in BG11 medium, respectively. Under the optimal NaCl concentration of 2.63 g/L, the highest lipid content (39.33%) was achieved, with the biomass concentration of 0.72 g/L, the total nitrogen removal efficiency of 39.00%, and the total phosphorus removal efficiency of nearly 100.00%, except for a higher total sugar content of 19.26% and total protein

content of 5.38%. In short, these results indicated that 2.63 g/L NaCl treatment was an efficient way to promote the lipid accumulation of *S. quadricauda* FACHB-1297 using xylose in papermaking waste liquid to produce biofuel.

- **Keywords:** Salinity stress; *Scenedesmus quadricauda*; Xylose mixotrophic cultivation; Biodiesel

**Priscilla de Souza Almeida, Camila Aparecida de Menezes, Franciele Pereira Camargo, Isabel Kimiko Sakamoto, Maria Bernadete Amâncio Varesche, Edson Luiz Silva. *Thermophilic anaerobic co-digestion of glycerol and cheese whey – Effect of increasing organic loading rate.* Pages 895-907.**

The organic loading rate (OLR) is one of the variables that directly affects anaerobic digestion. An increase in OLR can improve methane production, but it can also lead to process failures. Therefore, determining the proper OLR for the process is of great importance. This study analyzed the effect of increasing the OLR on cheese whey and glycerol co-digestion in a thermophilic anaerobic fluidized bed reactor (AFBR) by varying both the influent concentration and the hydraulic retention time (HRT). The increase in OLR from 5 to 20 gCOD.L<sup>-1</sup>.d<sup>-1</sup> was initially performed by increasing the influent concentration from 5 to 7.5, 10, 15, and 20 gCOD.L<sup>-1</sup>, at HRT of 24 h. Organic matter removal (87.7%), methane yield (MY) (253.0 mL CH<sub>4</sub>.gCOD<sup>-1</sup>rem), and methane production rate (MPR) (3.2 L CH<sub>4</sub>. L<sup>-1</sup>.d<sup>-1</sup>) showed the best performance at 10 gCOD.L<sup>-1</sup>.d<sup>-1</sup>. Conversely, raising the OLR to 20 gCOD.L<sup>-1</sup> enhanced the buildup of volatile fatty acids, resulting in a 38.5% decrease in MY. Based on these findings, the HRT was reduced from 24 h to 20 h and 16 h at influent concentration of 10 gCOD.L<sup>-1</sup> resulting in OLR of 10, 12, and 15 gCOD.L<sup>-1</sup>.d<sup>-1</sup>, respectively. The HRT at 20 h (12 gCOD.L<sup>-1</sup>.d<sup>-1</sup>) provided the highest MY values (around 292.5 mL CH<sub>4</sub>.gCOD<sup>-1</sup>rem), while the maximum MPR was observed at 16 h (5.1 L CH<sub>4</sub>. L<sup>-1</sup>.d<sup>-1</sup>). The main metabolites observed in all conditions were acetic acid (31.1–66.8%) and propionic acid (10.9–61.5%). The OLR also affected the microbial community, with Proteobacteria accounting for 53.1% of the relative abundance at 5 gCOD.L<sup>-1</sup>.d<sup>-1</sup> while Firmicutes accounted for 76.6% at 10 gCOD.L<sup>-1</sup>.d<sup>-1</sup>. At 10 gCOD.L<sup>-1</sup>.d<sup>-1</sup>, with maximum MY, the bacteria observed with the highest relative abundance were an unidentified genus of Lentimicrobiaceae (8.9%), "Blvii28 wastewater sludge group" (2.9%), and *Tolomonas* (1.4%). The archaea identified with the highest relative abundance at both OLRs (5 and 10 gCOD.L<sup>-1</sup>.d<sup>-1</sup>) was hydrogenotrophic *Methanobacterium* (27.3% and 2.6%, respectively).

- **Keywords:** Anaerobic fluidized bed reactor; Methane production; *Methanobacterium*

**Yuman Yao, Yiyang Dai, Jinsong Zhao. *An enhanced dynamic artificial immune system based on simulated vaccine for early fault diagnosis with limited data.* Pages 908-919.**

Artificial immune system (AIS) shows better performance with less training data in the process safety and risk engineering. However, the traditional AIS based fault diagnosis model is invalid for new process with no history data. Meanwhile, the data-based method has the limitation. To improve the process safety of chemical system under the extreme absence of data, an enhanced dynamic artificial immune system based on simulated vaccine and correlation coefficient methods (SV-CCDAIS), has been proposed. First, simulated vaccine was used to obtain the simulated data from simulation software or modelling for online diagnosis of actual process. Second, dynamic time warping was used to align the normal process data to solve the problem of time dimension misalignment. Third, different dynamic correlation measurement methods were proposed. Finally, a

complete diagnostic and autonomous updating process was designed. The proposed method was applied to an ethanol-water separation start-up process, results confirmed that the proposed method exhibited 1.5 time higher fault diagnosis accuracy compared to the convolutional neural network method based on dynamic kernel principal component analysis, in addition, and the average time of fault diagnosis is 5 s, which is shorter than comparative method.

- **Keywords:** Early fault diagnosis; Artificial immune system; Simulated vaccine; Start-up process

**Qiming Mao, Dongning Wei, Binghua Yan, Shuang Luo, Thomas William Seviour, Zongsu Wei, Xiande Xie, Lin Luo. *Removal of manganese in acidic solutions utilizing *Achromobacter* sp. strain QBM-4 isolated from mine drainage.* Pages 920-928.**

Biological approaches with the core of manganese-oxidizing bacteria (MnOB) are cheap and environmentally friendly solutions for the removal of bivalent manganese (Mn(II)). These bacteria typically worked well in the pH range of 5.5 – 8.0 but poorly under pH below 5.5. In this study, we isolated an acid-tolerant manganese-oxidizing bacterium (*Achromobacter* sp. strain QBM-4) from acid mine drainage (AMD), which was effective for Mn(II) removal at pH 4.0. Under optimized treatment conditions (i.e., 60.0 mg·L<sup>-1</sup> Mn(II), 100.0 mg·L<sup>-1</sup> Fe(III), and 35.0 °C), the Mn(II) removal efficiency reached 93.6 ± 0.8% at an initial pH of 4.0. Approximately 68.0% of the Mn(II) was removed through adsorption, and the remainder was attributed to oxidation. The Mn(II) oxidation rate was ~ 0.05 mM·d<sup>-1</sup> (initial pH of 4.0), comparable with other MnOB performing under near-neutral solutions. Ferric ions (Fe(III)) can form amorphous iron hydroxides, facilitating sorptive removal and catalytic oxidation of Mn(II). In contrast, ferrous ions (Fe(II)) reductively dissolve manganese oxides, inhibiting Mn(II) removal. A mechanism for the biological removal of Mn(II) was proposed, and the performance of *Achromobacter* sp. strain QBM-4 was further verified in three types of mine drainage.

- **Keywords:** Manganese removal; Acid resistance; Manganese-oxidizing bacteria; Acid mine drainage

**Ruipeng Tong, Xiaolong Wang, Lulu Wang, Xiangyang Hu. *A dual perspective on work stress and its effect on unsafe behaviors: The mediating role of fatigue and the moderating role of safety climate.* Pages 929-940.**

Work stress has a significant impact on unsafe behaviors. However, there has been limited exploration of the relationship between work stress and unsafe behaviors. The aim of this research was to examine the effect of work stress on unsafe behaviors, while incorporating the mediating effect of fatigue and the moderating role of safety climate. Data were collected from 1224 front-line oil workers in China. The findings showed that work stress had a significant effect on unsafe behaviors, and that fatigue and safety climate played partial mediating and moderating roles in the relationship respectively. In terms of their sub-dimensions, (1) job certainty and job control had positive influences on unsafe behaviors, while only social support was negatively associated with unsafe behaviors. (2) Five sub-dimensions of safety climate moderated the effect of work stress on unsafe behaviors. This research contributes to the study on the mechanism of unsafe behaviors by demonstrating differential effects of work stress, fatigue and safety climate and by considering their combined effects. Measures for reducing unsafe behaviors from the perspective of work stress and safety climate are discussed.

- **Keywords:** Oil workers; Work stress; Unsafe behaviors; Fatigue; Safety climate

**Syed Turab Raza, Jianping Wu, Eldon R. Rene, Zulfiqar Ali, Zhe Chen. *Application of wetland plant-based vermicomposts as an organic amendment with high nutritious value. Pages 941-949.***

The main aim of this study is to highlight the operational advantages of vermicomposting technology by reusing wetland plants and manure. An experiment with a full factorial design was conducted to investigate the effects of different vermicompost of wetland plants, including *Canna indica* (CiV), *Cyperus alternifolius* (CaV), *Acorus calamus* (AcV) and *Hydrocotyle vulgaris* (HvV), on maize growth. The vermicompost effects were compared with the conventional synthetic fertilizers (NPK) and the control treatment without any fertilizer (CK). Among the four species, CiV-vermicompost as an organic fertilizer showed the highest total nitrogen (1.45 g kg<sup>-1</sup>), soil organic matter (28.6 g kg<sup>-1</sup>), soil electrical conductivity (84.4  $\mu\text{s}=\text{cm}^{-1}$ ) and shoot biomass (265.1 g) compared with NPK and CK. This study revealed wetland plants can be used as organic amendments and offers a novel approach by reusing the ecological wastes to promote the transformation of nutrient-rich organic fertilizers and crop productivity while reducing the environmental pollution.

- **Keywords:** Vermicompost; Wetland plant; Nutrients; Resource recovery; Biomass utilization

**Thi Thuong Nguyen, He Huang, Thi An Hang Nguyen, Satoshi Soda. *Recycling clamshell as substrate in lab-scale constructed wetlands for heavy metal removal from simulated acid mine drainage. Pages 950-958.***

This study aimed to evaluate the feasibility of clamshells as a substrate in constructed wetlands (CWs) for removing heavy metals from acid mine drainage (AMD). Column-type CWs (ID 12.5 cm, H 50 cm) filled with clamshells or gravel were planted with cattails. Synthesized AMD containing 20 mg/L zinc (Zn), 0.3 mg/L cadmium (Cd), 20 mg/L copper (Cu), 1.1 mg/L lead (Pb), 0.6 mg/L manganese (Mn), and other minerals (pH=4.1) was fed to CWs (1 L/column) with hydraulic retention times of 2–7 days in sequencing batch mode. Results indicated higher metal removal in clamshell-based CWs with the pH neutralization than in gravel-based CWs. The removal efficiencies were 85.3–92.6%, 84.1–98.3%, 96.5–99.7%, 98.3–99.1%, and 64.0–83.8%, respectively, for Zn, Cd, Cu, Pb, and Mn. During 6 months of operation, 790.7 mg of Zn, 10.6 mg of Cd, 762.4 mg of Cu, 40.1 mg of Pb, and 19.9 mg of Mn were fed to each CW. Of those, retaining in the substrate was the main metal removal route, representing 49.7–82.5%, followed by plant uptake (16.1–39.0%), and other processes (0.6–3.2%). The metal contents in the clamshell were increased, although that of calcium was lowered after treatment. The clamshell-based CWs extended the cattail root and incubated sulfate-reducing bacteria in a larger population. These findings suggest a recycling way of seashells as filter media in CWs for heavy-metal-rich wastewater treatment.

- **Keywords:** Acid-mine drainage; Clamshell; Constructed wetland; Heavy metals, Sequencing batch mode

**Xinhong Li, Jingwen Wang, Guoming Chen. *A machine learning methodology for probabilistic risk assessment of process operations: A case of subsea gas pipeline leak accidents. Pages 959-968.***

Subsea gas pipeline leak may cause the catastrophic consequences, e.g., offshore fire and explosion, and the overturning of floating offshore structures. Efficient risk assessment is critical to prevent the unexpected offshore accident due to subsea gas pipeline leak. The modern technology advancement urges the need for developing new risk assessment approach in the case that a large volume of data becomes available. A new methodology comprising of BRANN implemented with BN is proposed for dynamic

risk assessment of process operations, which can capture the nonlinear and the non-sequential features of accident escalation. BN is used to model the accident scenario from causations to consequences considering the conditional dependencies among accident contributory factors. Subsequently, BN model as an informative base is mapped into BRANN model. The data-driven nature makes it better to capture the uncertainty among the cause-consequence relationships. The practicability of the methodology is illustrated by a case study of subsea gas pipeline leak accident. It is observed that BRANN model is superior in the network performance and prediction accuracy. This methodology can help to perform more effectively real-time risk assessment of process operations.

- **Keywords:** Subsea gas pipeline; Dynamic risk assessment; BN; BRANN; Process operations

**Miao He, Xin Chen, Mingbiao Xu, Huan Chen. *Inversion-based model for quantitative interpretation by a dual-measurement points in managed pressure drilling. Pages 969-976.***

Deep wells control safety problems have always been the focus of attention due to the influence of complicated geological conditions, such as high-temperature and high-pressure (HTHP). Considering the mathematical model is only approximation of reality, thus the continuous transmission of real-time measurements is more popular, which can be used to identify the undetermined downhole parameters and improve accuracy of the model predictions. In the current study, we use two pressure while drilling tools to monitor downhole parameters in real time. Firstly, combined with the unscented-Kalman-filter (UKF) algorithm, a well hydraulics forward model with density factor and friction factor based managed-pressure-drilling (MPD) system is developed to quantitatively analyze the actual transient annular pressure. Secondly, a new multi-phase flow inversion model is established by determining the inversion parameters as gas kick rate and the position of the gas kick, which is used to track the values of pressure and outlet flow rate in real-time. The results of the case indicate that the inversion accuracy of the inversion parameters increases with the distance between dual-measurement points, and the reasonable value is selected as 30 m. Additionally, the proposed model is successfully validated using synthetic data and experimental data, where the maximum errors in predicting the position of the gas kick are only 3.1% and 5.3% when tuning the model stably tends towards the true value, respectively. The proposed model achieves accurate quantitative interpretation and analysis of downhole gas kick conditions, further clarifies the previously unknown key parameters of downhole gas kick, and has important significance for the realization of safe and efficient drilling.

- **Keywords:** Unscented kalman filter; Dual-measurement points; Managed pressure drilling; Multi-phase flow; Gas kick

**Nurul Shuhada Mohd Makhtar, Juferi Idris, Mohibah Musa, Yoshito Andou, Ku Halim Ku Hamid, Siti Wahidah Puasa. *High lead ion removal in a single synthetic solution utilising plant-based *Tacca leontopetaloides* biopolymer flocculant (TBPF). Pages 977-986.***

The present study aimed to remove lead ions (Pb<sup>2+</sup>) in a single synthetic solution by employing a plant-based *Tacca leontopetaloides* biopolymer flocculant (TBPF). The ions were eliminated through the flocculation process via the Jar test experiment. The maximum Pb<sup>2+</sup> removal was determined based on one-factor-at-a-time (OFAT) and central composite design (CCD). Based on the OFAT, the maximum Pb<sup>2+</sup> eliminated, 83%, was achieved at pH 6 synthetic solution, 2.5 mg/L initial Pb<sup>2+</sup> concentration, and 3% initial TBPF concentration at 192 mg/L dosage. The highest Pb<sup>2+</sup> removal of 73% was recorded at pH 6.4 synthetic solution with 11.8 mg/L initial Pb<sup>2+</sup> concentration at a constant 3% initial TBPF concentration and 192 mg/L TBPF dosage when the CCD was

employed. The excellent Pb<sup>2+</sup> removal with the environmentally friendly plant-based TBPF utilised in the current study demonstrated outstanding potential in industrial heavy metal treatments, particularly at the primary stages.

- **Keywords:** Pb ion removal; Central composite design; One-factorial-at-a-time; *Tacca leontopetaloides* biopolymer flocculant